Master's Report

Recruitment of Tendon Crimp with Applied Tensile Strain

Kristi Ann Hansen

2000

Recruitment of Tendon Crimp with Applied Tensile Strain

by

Kristi Ann Hansen

A Manuscript and Supplemental Materials Submitted to the Faculty of the

BIOMEDICAL ENGINEERING IDP

In Partial Fulfillment of the Requirements
For the Degree of

MASTER OF SCIENCE
WITH A MAJOR IN BIOMEDICAL ENGINEERING

In the Graduate College

THE UNIVERSITY OF ARIZONA

2000

Contents

Recruitment of Tendon Crimp with Applied Tensile Strain

Kristi A. Hansen*, Jeffrey A. Weiss[+], Jennifer K. Barton*

*Biomedical Engineering Program
The University of Arizona
1230 E. Speedway Blvd.
Tucson, AZ 85721

[+]Department of Bioengineering
The University of Utah
50 S Central Campus Dr #2480
Salt Lake City, UT 84112

In Preparation, *Journal of Biomechanical Engineering*
August 8, 2000

Keywords: collagen, fascicle, fibril, optical coherence tomography, material properties

Corresponding Author:

Jeffrey A. Weiss, Ph.D.
University of Utah
50 S. Central Campus Drive, Room 2480
Salt Lake City, Utah 84112
Phone: 801-581-8528
FAX: 801-585-5361
Weiss@barney.bioen.utah.edu

Abstract

The stress-strain behavior of ligaments and tendons begins with a toe region that is believed to result from the straightening of crimped collagen fibrils. Their physiological function is mostly confined to this toe region and changes in crimp morphology are believed to be associated with pathological conditions. A relatively new imaging technique, optical coherence tomography (OCT), provides a comparatively inexpensive method for nondestructive investigation of tissue ultrastructure with resolution on the order of 15 μm and the potential for use in a clinical setting. The objectives of this work were to measure the period of crimp pattern in rat tail tendon fascicles, and to measure changes in crimp period as a function of tensile strain using OCT. Fascicles from rat tail tendons were subjected to 0.5% strain increments up to 5% and imaged at each increment using OCT. The OCT images corresponded well to OM images taken between crossed polarizing lenses. Crimp pattern disappeared completely at strains below 3%, first near the surface of the fascicle and finally at the center. Average crimp period increased as strain increased, but individual, axially aligned periods increased and decreased due to non-uniform recruitment of crimp.

Introduction

The relationship between tissue microstructure and continuum level function has long been a topic of interest in biomechanics and tissue engineering. The material properties of biological tissues depend on the component materials and structural organization from the microscopic to macroscopic level. Due to difficulties in accurately visualizing tissue microstructure, studies of structure-function relations in biological soft tissues are often difficult or impossible. Although histological methods can provide some microstructural information, these techniques require destruction of the tissue and often alter the relationship between tissue components.

The material behavior of tendons and ligaments is important in the study of injury, reconstruction, and surgical techniques. Knowledge of the tissue structure and organization can enhance this understanding. Although there are subtle differences in the organization of different tendons and ligaments, the rat tail tendon has been studied extensively as a model tissue. Tail tendons are composed of several fascicles, which in turn consist of fibrils (Kastelic et al. 1978, Niven et al. 1982, and Rowe 1985). A crimp, or banding pattern can be readily observed in histological preparations of rat tail fascicles via polarized light microscopy. Rigby et al. (1959) and Diamant et al. (1972) observed that crimp pattern disappears below 4% strain. The stress-strain behavior of fascicle is non-linear prior to the extinction of the crimp, forming a "toe region" in the stress-strain curve. The physiological function of tendon is mostly confined to this toe region (Viidik et al. 1982).

Several models of structural organization have been proposed for the rat tail tendon. Diamant et al. (1972) used optical microscopy (OM) to demonstrate the planarity of a zigzag crimp waveform inherent in fascicle fibrils. Kastelic et al. (1978) proposed that fascicles have a cylindrical array of planar zigzag crimped fibrils based on interpretation of OM and scanning

electron microscopy (SEM) studies. Niven et al. (1982) presented a structural model based on a triangular cross-sectional shape with planes of crimped fascicles packed parallel to the longest edge of the triangle. Rowe (1985b) used OM and SEM to develop a rat tail tendon fascicle model that suggested that the waveforms of collagen fibrils assemble side-by-side with a degree of freedom in any direction in the register of the wave. Regardless of the exact fibril organization, all previous investigations are in agreement that the fascicles form a wavy configuration, or crimp pattern, with variable periodicity. Studies have also demonstrated that the band width seen in OM pictures is directly related to the crimp period measured using histological techniques (Rigby et al. 1959, Gathercole and Keller 1991). Gathercole and Keller summarized their 18 years of work by noting that "alterations in crimp structure are symptoms, or even causes, of pathological conditions."

In addition to OM, a number of non-destructive techniques have been applied to the quantification of soft tissue microstructure. Sacks et al. (1997) used a small angle light scattering device to measure fiber orientation in planar fibrous connective tissue of less than 500 μm thickness with an angular resolution of approximately 1 degree and a spatial resolution of ±254 μm. Magnetic resonance diffusion tensor microscopy was used to measure fiber orientation in canine myocardium (Hsu et al. 1998) and the lamellar structure of the intervertebral disc (Hsu and Setton 1999). Caspers et al. (1998) used Raman spectroscopy to investigate the composition of the layers of skin. Optical Coherence Tomography (OCT) provides a relatively inexpensive, non-destructive alternative for the analysis of soft tissue microstructure, with resolution that is superior to the aforementioned techniques in three dimensions (on the order of 15 μm) (Huang et al. 1991). OCT is an optical analogue to ultrasound, utilizing reflected near-infrared light instead of sound. The intensity of reflected low coherence light is measured, using a Michelson interferometer to determine its spatial origin.

OCT has been used to image many biological tissues *in vitro* and *in vivo*, including skin (Schmitt et al. 1995, and Barton et al. 1997), aorta (Brezinski et al. 1996) and tendon (de Boer et al. 1997).

Nondestructive and minimally invasive measurement of the ultrastructure of collagenous soft tissues would provide a unique method for the evaluation of normal and healing tissues and the efficacy of treatment regimens. The technique could also be used to determine microstructural parameters for constitutive models of the tissue material behavior (Kwan et al. 1989; Hurschler et al. 1997). The objectives of this work were to assess the period of the crimp pattern in rat tail tendon fascicles, and to measure changes in crimp period as a function of tensile strain using OCT. Our hypotheses were that (1) the width of crimp bands would increase and the bands would eventually disappear as increasing axial strain was applied, and (2) the average period of sequential, axially aligned crimp bands would increase with increasing strain.

Materials and Methods

Experimental design and tissue preparation. Eight fascicles from five rat tails were imaged with OCT at successive levels of uniaxial tensile strain. Rat tails were obtained immediately following sacrifice, wrapped in 0.9% buffered saline wetted gauze, and frozen at –70°C until dissection. Thawed tails were skinned and cut approximately 65 mm from the proximal end. Sections of single fascicles were gently teased from the surrounding epitenon (Rowe 1985) and clamped into a custom built mechanical testing device (Fig. 1). To preserve the mechanical and optical properties of the tissue, fixatives were not used and fascicles were kept continuously moist with 0.9% buffered saline during harvest, preparation, and imaging. A single monofilament suture (Polyglyconate, 3-0, Davis & Geck Monofil Inc., Manati, PR) was attached with cyanoacrylate to each fascicle, transverse to the collagen fiber direction of the tissue in the center third of the fascicle length (Fig. 1, inset). The suture served as a fiduciary for

registration between successive OCT images. Fascicle ends were wrapped in saline-soaked gauze to increase the gripping area and avoid tissue damage. Each fascicle end was secured in a clamp, allowing a small amount of slack to avoid prematurely stretching the tissue. The mechanical test device was then attached to the motorized stage for OCT imaging.

OCT System. The OCT system used in this study used a short coherence length source, in this case a superluminescent diode, with a center wavelength of 1290 nm and a bandwidth of 49 nm (Figure 2). This was coupled with a red aiming beam and directed into one arm of a fiber Michelson interferometer. This light was split into reference and sample arms. In the sample arm, light was focused onto the tissue. In the reference arm, pathlength modulation was provided by a galvanometer-mounted retroreflector. Light reflected from the reference and sample arms interfered only when the respective pathlengths were within a source coherence length (approximately 16 μm). Thus by scanning the retroreflector, a determination of reflectivity vs. sample depth (an a-scan) was made. This signal was detected by a photodiode, with an interference fringe frequency dependent upon the speed of the moving retroreflector. A lock-in amplifier demodulated the signal at this frequency and allowed signals weaker than 10^{-10} of the incident light to be detected. A two-dimensional image was created from multiple a-scans acquired while a motorized stage translated the tendon in the lateral direction. The system axial and lateral resolution, given by the coherence length of the source and the sample beam focus in tissue, was 16 μm and 14 μm respectively. Images consisting of 200 a-scans were obtained in approximately 14 seconds.

Mechanical test device and protocol. The mechanical test device was designed to apply measured increments of uniaxial strain to the fascicles. One clamp was attached to a translation stage and the other was fixed to a stationary plate. A micrometer (accuracy ±5 μm) adjusted the position of the translation stage to apply strain to the clamped tissue. A 2.5 lb. load cell

(Transducer Techniques, Temecula, CA, accuracy ±0.055 N) was used to continuously monitor applied load during the application of each strain increment.

The zero-load length of the fascicle was established by consecutively applying and removing a small tare load (0.01 N) via adjustment of the micrometer. The clamp-to-clamp distance was then measured with calipers (accuracy ±50 μm) to determine the zero-load length (l_0). Three OCT images were then taken perpendicular to the fascicle long axis and in the center third of the fascicle length. These images were processed using Scion Image (Scion Corporation, Frederick, MD) to determine cross-sectional area of the fascicle with the assumption of elliptical cross-sectional shape. The three measurements were averaged to determine initial cross-sectional area (A_0). The mechanical test device was then rotated 90° and an OCT image of the tissue was acquired parallel to the fascicle long axis in the zero-load configuration.

The fascicle was consecutively stretched in increments of approximately 0.5% clamp-to-clamp strain. The exact incremental change in length (Δl) was recorded in order to calculate clamp-to-clamp engineering strain as $\varepsilon = \Delta l / l_0$. An OCT image was acquired for each strain increment once the load relaxation rate dropped below a value of 0.001 N/sec. All longitudinal images included the suture fiduciary. Engineering stress (σ) was calculated at each strain increment using the initial cross-sectional area (A_0) and the measured load (F) at the beginning of each image acquisition as $\sigma = F/A_0$. To determine any differences between clamp-to-clamp strain and tissue level strain, a pilot study was performed using a series of surgical microscope images from single fascicles. The fascicles were placed in the mechanical test device and subjected to the same incremental strain conditions described above. Clamp-to-clamp values of l_0 and Δl were measured as previously stated. In these images the fascicles did not have suture markers but the center third was identified by two thin marks of black stain. Marker-to-marker

L_0 and ΔL were measured from the images. The difference between the two strain measures was smaller than lateral resolution of the OCT system.

Band pair relationship to crimp period. To determine the relationship between banding and crimp period observed in OM studies (Diamant et al. 1972, Rigby et al. 1959, Gathercole and Keller 1991) and banding observed in OCT images, three fascicles were obtained from a single rat tail and imaged using OCT and subsequently using an optical microscope (Nikon, SMZ-2T) between cross polarizers. Each fascicle was adhered to a microscope slide at each end with cyanoacrylate, such that the fascicle was visibly taut. Two monofilament sutures were attached with cyanoacrylate, 4 mm apart and perpendicular to the long axis of the fascicle in the center of the length between adhesion spots. These sutures served as fiduciaries for registration between corresponding OCT and OM images. The fascicles were kept in a 0.9% buffered saline bath at all times.

Longitudinal OCT images were taken along the center of the fascicle with the slide in two separate orientations. One image was taken with the slide perpendicular to the imaging beam axis and the second with the slide parallel to the beam axis. Two OM images were also obtained. The first was acquired such that extinction bands encompassed an entire crimp arm or half of a crimp period (Gathercole and Keller 1991), such that each OM image band pair width was equivalent to one full crimp period. The second image was taken with the polarizers crossed. These images were used to relate OCT image banding to OM image banding, which has a known relationship to crimp period to OM images. OM images and corresponding OCT images were compared visually, side-by-side. Perpendicularly acquired OCT images were compared by their average period.

Data reduction and statistical analysis. The OCT images were processed and analyzed using Adobe Photoshop (Adobe Systems Inc., San Jose, CA). A median filter with a radius of

one pixel was applied to each strain OCT image. A threshold value was then determined from inspection and applied consistently to all images from a single fascicle, converting the grayscale images to binary (black and white) images to clearly define the banding. For each OCT image taken in the zero-load configuration, a number of consecutive band pair widths (4 to 11) were identified and measured (Fig. 3) along the centerline. The measurement was repeated at each increment of strain for which any of the band pair widths were still visible. The average banding period was calculated at each strain level by summing the band pair widths and dividing by the number of visible band pairs. When a band pair disappeared between other pairs, a single measurement was taken across both previously visible pairs. A second average was calculated that excluded the "merged" measurements. A one-way repeated measures ANOVA was performed on all data for the first five strain increments (0 to 2%)(significance at $p \leq 0.05$).

Results

Stress-strain data from eight fascicles were successfully obtained for strain increments from 0% to 5% with the anticipated behavior. There was a strong correlation between the banding period seen in OCT images and the crimp period seen in OM images. Crimp data were continuously tracked at strain increments from 0% to a minimum of 1% and a maximum of 2.5%. These data provided insight into the behavior of crimp during uniaxial extension. Average crimp period increased until crimp disappeared while individual crimp periods both increased and decreased.

Stress-strain behavior. The stress-strain data exhibited the characteristic nonlinear behavior of collagenous soft tissues. At a given strain level, stress values were lower than the expected range reported in the literature (19 to 40 MPa at 5% strain, Betsch and Baer 1980, Price

et al. 1996) (Fig. 4). The toe region of the curve was longer than that documented in the study by Price et al.

Relationship between OCT and OM images. The appearance of OCT images was similar to OM images, in that both show a banding with variable period. Side-by-side comparison of the OCT bands and OM bands revealed a two-to-one relationship. At each transition from a light to dark or a dark to light band in an OM image, a bright band appeared in the OCT image (Fig. 3). Average OCT band measurements from images taken with the slide parallel and perpendicular to the imaging beam axis differed from each other by less than the resolution of the OCT system.

Individual crimp changes with applied strain. Crimp periods began to disappear individually rather than simultaneously along the length of the fascicle or successively from the ends toward the center, as might be expected if strain distribution was higher towards the clamped ends. Intermittently, single periods disappeared before the whole. Banding at the surface of the fascicle disappeared sooner than along the center axis. Non-uniform variations in single crimp periods occurred in each straining sequence, both increasing and decreasing.

Average crimp changes with applied strain. Average crimp period was plotted against applied strain to determine the correlation between strain level and crimp period. As strain increased, the average crimp period also increased (Fig. 5). The average increase was nonlinear when all data were considered. When measurements for periods that had merged with other periods were omitted from the average, the increase in the average was still non-linear, but the curve was smoother. The data point at 2.5% strain is not shown since only three period measurements were available at this strain level.

Discussion

This study utilized OCT imaging to measure changes in during uniaxial extension. The comparison of OCT and OM images facilitated the interpretation of the OCT bands in relation to crimp period. The results may also aid the mathematical modeling of ligament and tendon behavior.

It is difficult to accurately determine the initial onset of stress and strain when testing tissues as small as tendon fascicles (approximately 300 microns in diameter). Kastelic et al. (1980) reported that stress at the beginning of the stress-strain curve is of such low magnitude that there is ambiguity, even with very sensitive load transducers. This may explain the differences between the reported stress-strain values in the literature. Kastelic considered the beginning point to be when the specimen first appeared to be taut. Others (Price et al. 1996) began their measurements once the crimp disappeared. The present study demonstrated that small loads were distinguishable just before the fascicle appeared taut. It is not surprising that our stress data for the strains measured is lower than reported in the literature, considering these observations. This also explains the long appearance of the toe region in our data in comparison with the literature. If the data reported by Price et al. (1996) is adjusted to consider for an additional 2% strain experienced prior to removing crimp, then the two data sets are in agreement.

OM studies of fascicle crimp have shown that image banding occurs due to the orientation of the fibrils in relation to the incident light (Gathercole and Keller 1991). A similar phenomenon occurs in OCT images. The comparison between OCT and OM images helps explain how the OCT imaging beam interacts with the crimped fibrils. OCT depends on reflected light rather than transmitted light. The results indicate, as expected, that more light is reflected when the fibrils are aligned perpendicular to the beam. Strong reflections consequently

occur at the crests and troughs of the crimp waveform. The band period measured in OCT images is therefore equivalent to half of a crimp period. Some variation between OCT and OM measurements of crimp period may occur due to the difference in the volume of tissue being imaged. An OM image is a projection of the whole tissue while an OCT image is a cross-section of the tissue with a thickness equal to the axial resolution (14 μm in this case). OM images produce an average of all crimp planes in the tissue. OCT images should be able to provide a more local measurement of crimp. The individual disappearance of crimp periods suggests that there is non-uniform recruitment of crimp along the length of the fascicle. This important observation needs further investigation as it may have significant implications in the understanding of mechanical behavior in the toe region. As mentioned in the introduction, Kastelic et al. (1978) suggested that fibrils are arranged in planes and cylindrically packed to form a fascicle and that the crimping plane for a given fibril is approximately normal to the radius from the fascicle center and that crimping angle decreases with decreasing radius. Kastelic et al. (1980) presented a model called SSL (sequential straightening and loading) based on the above morphological understanding, in which only straightened fibrils produce resistance to strain. In this model, he hypothesized that the inner fibrils straightened first, inducing the onset of the stress-strain curve, and sequential straightening occurred toward the outer edge of the fascicle. He assumed that crimped fibrils had negligible resistance to extension. Our observations agree with a radially sequential fibril straightening theory, only the sequence of straightening appears to be from the outside toward the center (Fig. 6), leaving the center crimp visible the longest. Our observations support a structural composition theory of cylindrically packed fibril planes, based on the ability to consistently and easily obtain an image with banding that was continuous across the width of the fascicle without preferentially choosing a specific rotational orientation about the long axis of the fascicle. Our observations also indicate that

fascicle cross section is elliptical in the "free" (removed from epitenon) state, as opposed to circular or triangular.

The average crimp period changes calculated for all data is higher than is physically possible, assuming very small crimp angles (less than 25 degrees, Diamant et al. 1972), if no elongation, or very little, occurs in the fibrils before the crimp disappears. This is due to the method of measuring across two periods that appear to merge into one large period while only accounting for the one period measurement in the average. When merged period measurements were removed from the average calculation, the increase in the average was much smaller and more realistic. The change in average period between 0% strain and 2.0%, beyond which most crimp had disappeared, was about 20%. This suggests that crimp angles were close to 33 degrees.

Future work should include a more rigorous characterization of the interaction between a short coherence length light source and birefringent fibers of varying orientation. The ability to image from different rotations about the fiber axis is needed as well as a side-by-side comparison with OM at each strain level. Quantitative control of the polarization state of the incident light is also needed, although images taken with a polarization sensitive OCT (PS-OCT) system revealed that the appearance of banding is not altered when changing between perpendicularly oriented polarization states (unpublished data). Resolution is currently limited by the coherence length of the later source, but femtosecond lasers (Drexler et al. 1999) can improve resolution to 1-3 microns at a substantially increased cost for system construction.

This study has demonstrated that OCT is capable of visualizing crimp changes during uniaxial extension and that crimp period increases with applied strain in a non-linear fashion. It has also shown that crimp recruitment is non-uniform along the length of the fascicle and that complete straightening occurs from the outside of the fascicle toward the center. Future work

will include the study of stress relaxation behavior and the associated effects on crimp period, and volumetric imaging of fascicles under tensile strain.

Acknowledgements

Support by National Science Foundation grant #9978820 (JKB,KAH) and a Whitaker Foundation Transition Grant (JAW,KAH) is gratefully acknowledged.

References

Barton, J. K., Milner, T. E., Pfefer, T. J., Nelson, J. S., Welch, A. J., 1997, "Optical low-coherence reflectometry to enhance Monte Carlo modeling of skin," *Journal of Biomedical Optics*, **2(2)**:226-234.

Betsch, D. F., Baer, E., 1980, "Structure and mechanical properties of rat tail tendon," *Biorheology*, **17**:83-94.

Brezinski, M. E., Tearney, G. J., Brett, B. E., Boppart, S. A., Hee, M. R., Swanson, E. A., Southern, J. F., Fujimoto, J. G., 1996, "Imaging of coronary artery microstructure with optical coherence tomography," *American Journal of Cardiology*, **77**:92-93.

Caspers, P. J., Lucassen, G. W., Wolthuis, R., Bruining, H. A., Puppels, G. J., 1998, "In vitro and in vivo Raman spectroscopy of human skin," *Biospectroscopy*, **4(5 Suppl)**:S31-39.

de Boer, J. F., Milner, T. E., van Gemert, M. J. C., Nelson, J. S., 1997, "Two-dimensional birefringence imaging in biological tissue by polarization-sensitive optical coherence tomography," *Optics Letters*, **22**:934-936.

Diamant, J., Keller, A., Baer, E., Litt, M., Arridge, R. G. C., 1972, "Collagen; ultrastructure and its relation to mechanical properties as a function of ageing," *Proceedings of the Royal Society of London. Series B: Biological Sciences*, **180**:293-315.

Drexler, W., Morgner, U., Kartner, F. X., Pitris, C., Boppart, S. A., Li, X. D., Ippen, E. P. Fujimoto, J. G., 1999, "In vivo ultrahigh-resolution optical coherence tomography," *Optics Letters*, **24(17)**:1221-1223.

Gathercole, L. J., Keller, A., 1991, "Crimp morphology in the fibre-forming collagens," *Matrix*, **11**:214-234.

Hsu, E. W., Muzikant, A. L., Matulevicius, S. A., Penland, R. C., Henriquez, C. S., 1998, "Magnetic resonance myocardial fiber-orientation mapping with direct histological correlation," *American Journal of Physiology*, **274(5 Pt 2)**:H1627-34.

Hsu, E. W., Setton, L. A., 1999, "Diffusion tensor microscopy of the intervertebral disc anulus fibrosus," Magnetic Resonance in Medicine, **41**:992-999.

Huang, D., Swanson, E. A., Lin, C. P., Schuman, J. S., Stinson, W. G., Chang, W., Hee, M. R., Flotte, T., Gregory, K., Puliafito, C. A. et al., 1991, "Optical coherence tomography," *Science*, **254(5035)**:1178-1181.

Hurschler, C., Loitz-Ramage, B., Vanderby, R., Jr., 1997, "A structurally based stress-stretch relationship for tendon and ligament," *ASME Journal of Biomechanical Engineering*, **119**:392-399.

Kastelic, J., Galeski, A., Baer, E., 1978, "The multicomposite structure of tendon," *Connective Tissue Research*, **6**:11-23.

Kastelic, J., Palley, I., Baer, E., 1980, "A Structural Mechanical Model for Tendon Crimping" *Journal of Biomechanics*, **13**:887-893.

Kwan, M. K., Woo, S. L-Y., 1989, "A structural model to describe the nonlinear stress-strain behavior for parallel-fibered collagenous tissues," *ASME Journal of Biomechanical Engineering*, **111**:361-363.

Niven, H., Baer, E., Hiltner, A., 1982, "Organization of collagen fibers in rat tail tendon at the optical microscope level," *Collagen Related Research*, **2**:131-142.

Price, J. P., Njus, G. O., Conway, T. A., 1996, "Ultrastructural properties of rat tail tendon," Proceedings of the 1996 Fifteenth Southern Biomedical Engineering Conference., 456-459.

Rigby, B. J., Hirai, N., Spikes, J.D., Eyring, H., 1959, "The mechanical properties of rat tail tendon," *Journal of General Physiology*, **43**:265-289.

Rowe, R. W. D., 1985, "The structure of rat tail tendon," *Connective Tissue Research*, **14**:9-20.

Rowe, R. W. D., 1985b, "The structure of rat tail tendon fascicles," *Connective Tissue Research*, **14**:21-30.

Sacks, M. S., Smith, D. B., and Hiester, E. E., 1997, "A small angle light scattering device for planar connective tissue microstructural analysis," *Annals of Biomedical Engineering*, **25**:678-689.

Schmitt, J. M., Yadlowsky, M., Bonner, R. F., 1995, "Subsurface imaging of living skin with optical coherence microscopy," *Dermatology*, **191**:93-98.

Viidik, A. Danielsen, C. C., Oxlund, H., 1982, "On fundamental and phenomenological models, structure and mechanical properties of collagen, elastin and glycosaminoglycan complexes," *Biorheology*, **19**:437-451.

Figure Legends

Figure 1. OCT system schematic. Using Michelson interferometry, backscattered light from the sample and translating retroreflector interferes when the pathlength is within the coherence length of the source.

Figure 2. Mechanical testing device. Inset shows a close-up of the clamps with a fascicle secured between them.

Figure 3. OCT and OM comparison and measurement of crimp band period. The two images were obtained from the same location on a single fascicle. The top image is an OCT image and the bottom is from OM. The vertical arrows indicate that a bright band appears in the OCT image at the same location on the fascicle that a transition between light and dark bands occurs in the OM image. Measurements from OCT images were taken across each visible band pair as indicated by the horizontal arrow.

Figure 4. Average stress-strain curve for all fascicles tested.

Figure 5. Average crimp period vs. strain.

Figure 6. Sequence of OCT images. A) 0%, B) 0.5%, C) 1.0%, D) 1.5%, E) 2.0%, F) 2.5%. Bands begin to disappear on the outer edges first.

Figure 1

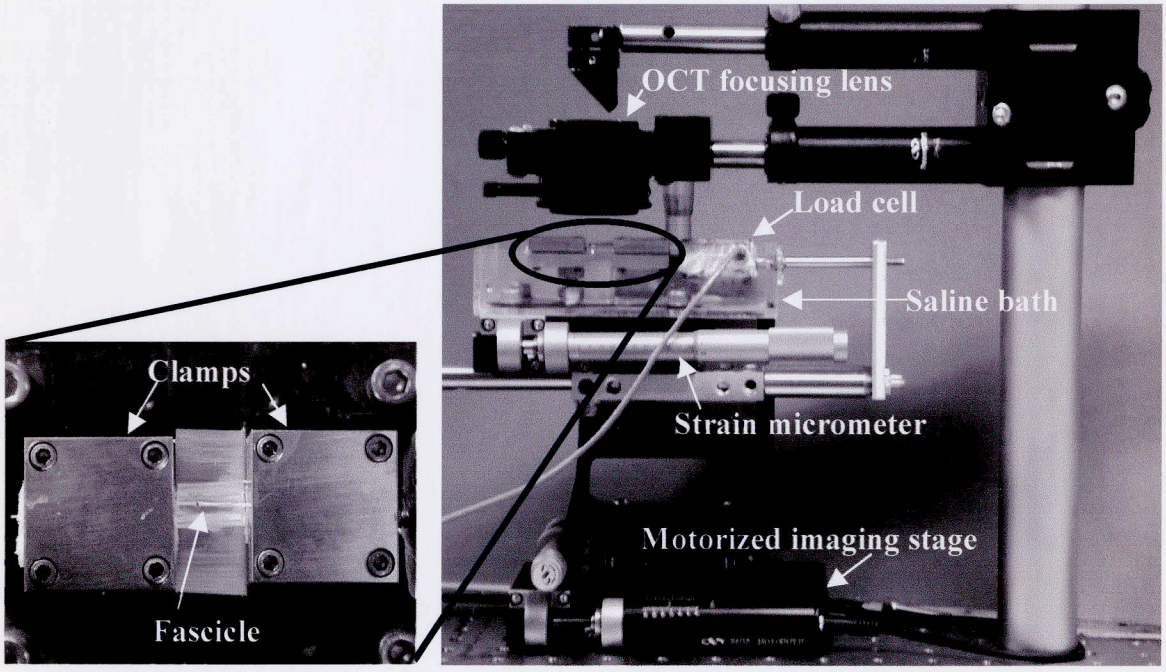
OCT focusing lens
Load cell
Saline bath
Strain micrometer
Motorized imaging stage
Clamps
Fascicle

Figure 2

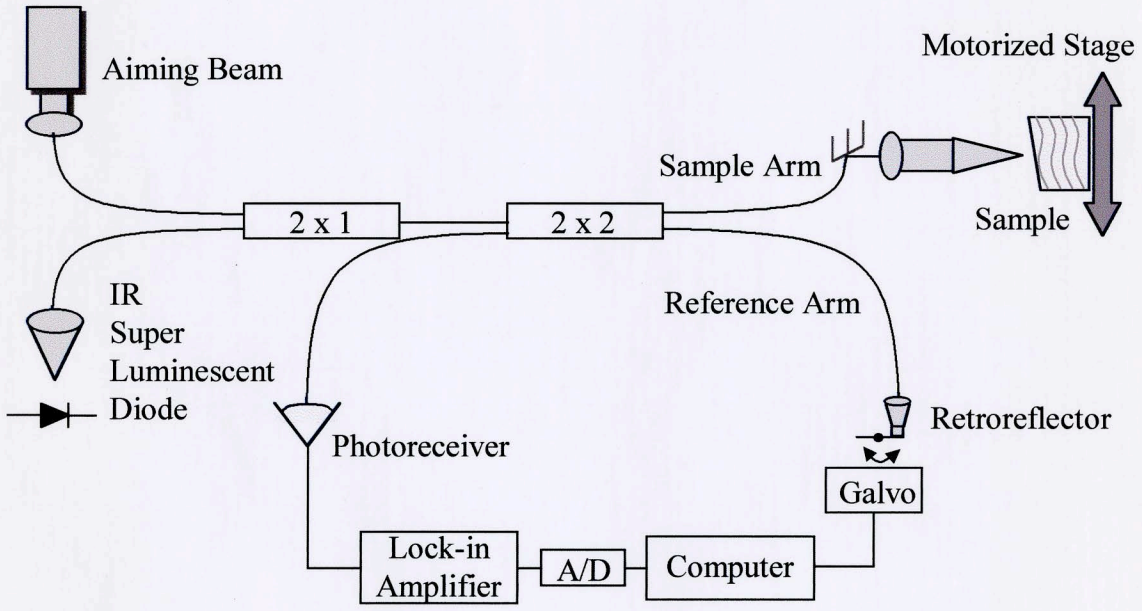
Aiming Beam
Motorized Stage
Sample Arm
Sample
2 x 1
2 x 2
IR
Super
Luminescent
Diode
Reference Arm
Photoreceiver
Retroreflector
Galvo
Lock-in
Amplifier
A/D
Computer

Figure 3

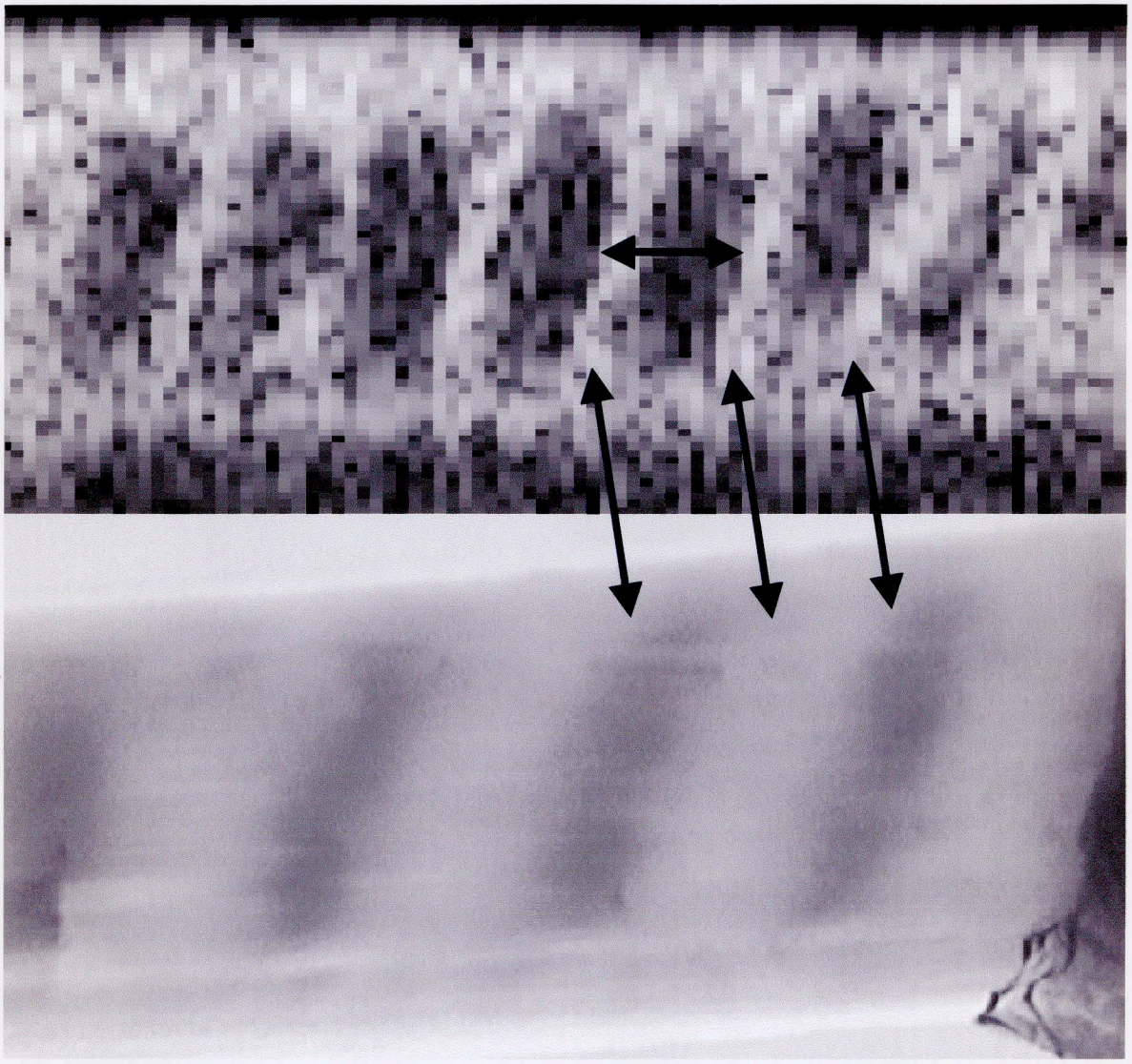

Figure 4

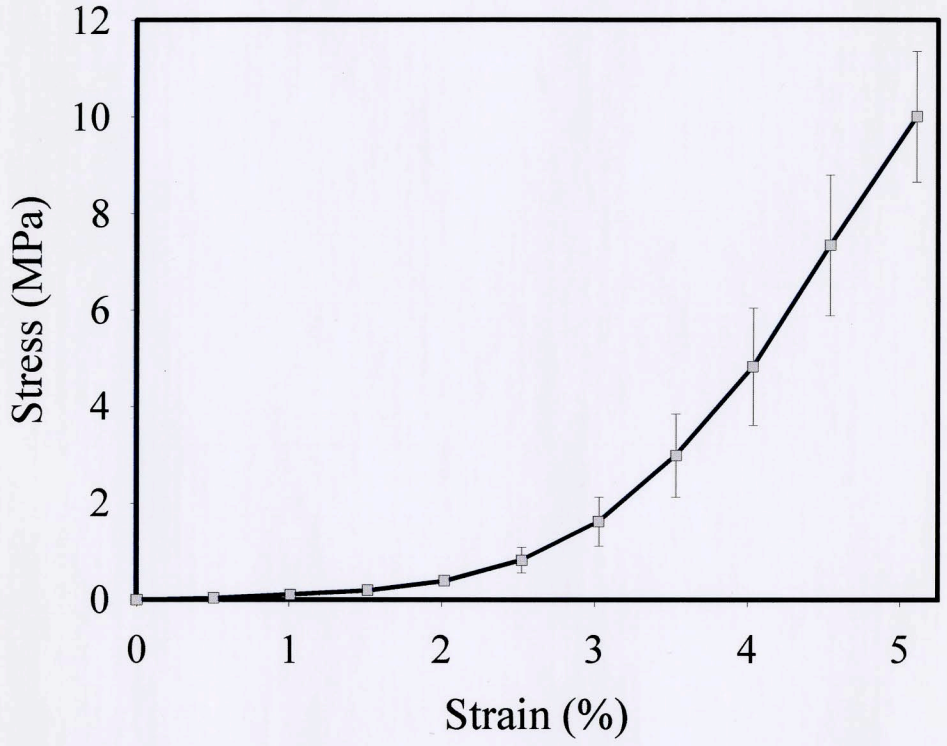

Figure 5

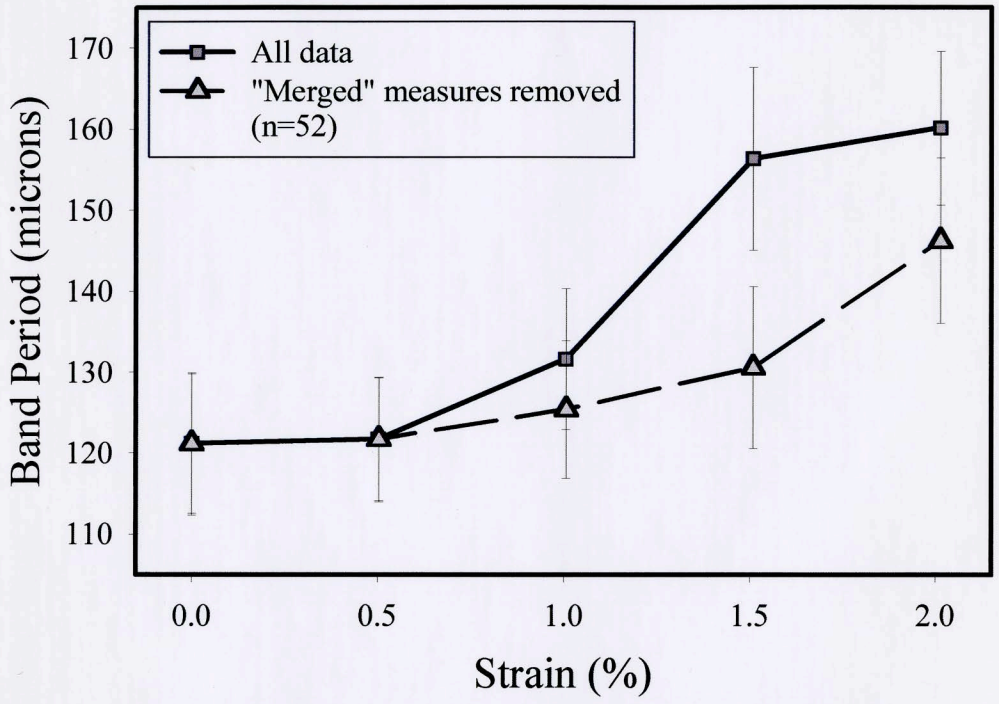
All data
"Merged" measures removed
(n=52)
Band Period (microns)
170
160
150
140
130
120
110
0.0
0.5
1.0
1.5
2.0
Strain (%)

Figure 6

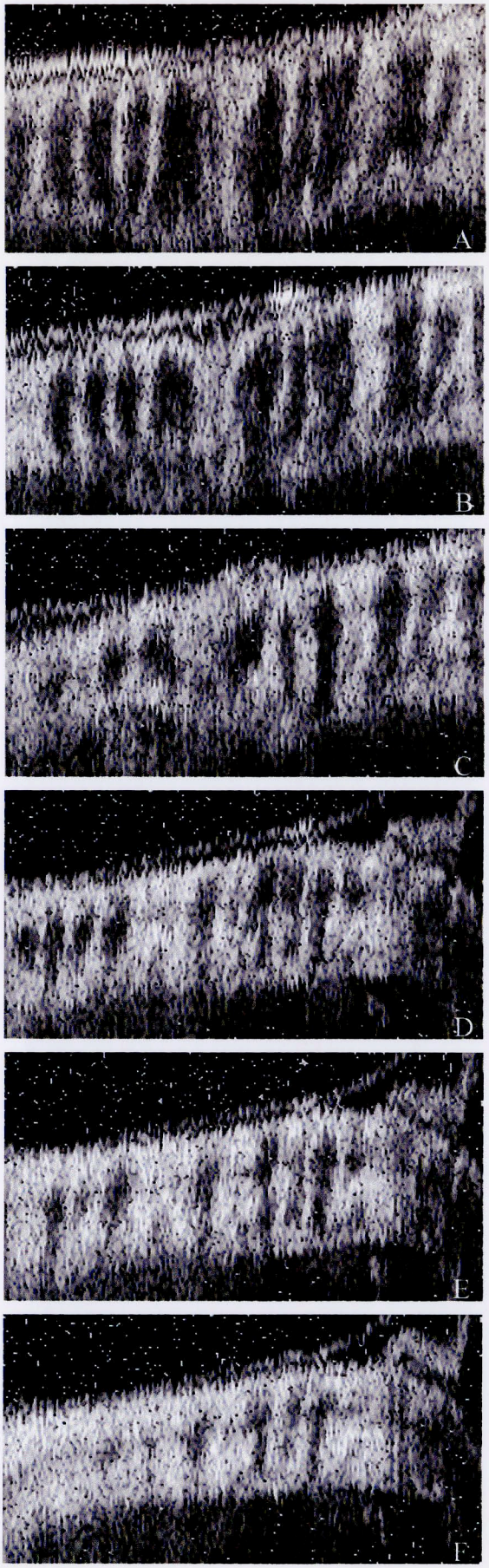

Appendix A - Tissue Clamping Technique

The clamps in the mechanical test device were originally designed to hold cow and sheep tendon or ligament. The gripping surface of the clamps was not as effective on these large tissues as was hoped and tissue sources (UA meat lab) were unreliable. Testing ceased on cow and sheep tendon before a suitable solution was found. Research was then concentrated on rat tail fascicles, which were clamped with much more success. Initially, the fascicles were gripped bare. The tissue was so small that it would sometimes slip between the clamps at higher strains. Next, small pieces of rubber were glued (cyanoacrylate) to the ends that were to be clamped to increase the contact area and hopefully help grip the tissue more consistently. This failed due to tissue hardening and failure at the glue site. The fascicles simply broke off next to the rubber or slipped between the rubber in spite of the glue. Finally, the fascicle ends were wrapped in saline soaked gauze. This proved successful. The procedure follows.

1) Remove the top clamp piece and place it aside.
2) Cut one inch square pieces of four-layer thick cotton mesh gauze.
3) Place one square of gauze on each clamp bottom.
4) Pour or pipette saline over the gauze.
5) Lay a single fascicle over the center of both clamp pieces, keeping it as straight as possible and without any twisting.
6) Adjust the micrometer such that there is enough slack in the tissue to prevent prematurely stretching it during further adjustments to the clamps.
7) Fold gauze in from both sides to cover the top of the tissue (the gauze should now be folded in thirds around the fascicle) and leave the clamp screw holes unobstructed.
8) Place the clamp tops, with each gripping area toward the opposite clamp.
9) Put four screws into place on each clamp, without tightening them.
10) Tighten each screw as far as you can with your fingers.
11) The screws must be tightened evenly the rest of the way, alternately tightening screws that are diagonally opposite with an allen wrench.

When a load cell is connected to the test device, care must be taken while tightening clamp screws to make sure that the load cell is not damaged by overloading.

Appendix B - Techniques For Marking Tissue

Marking tissue to be imaged under OCT is important if a second method of imaging, histology, or any treatment is to be applied to the tissue between images for comparison. I was concerned with the later. The treatment applied was strain, which requires that the markers be adhered to the tissue so that they will move with it. Some preliminary tests were performed on cow and sheep tendon and ligament, but the main tissue used was rat tail tendon fascicle.

Important things to consider when choosing a marking material for strain tests:

1) The material needs to intersect the scan of the imaging beam only briefly to attain optimal imaging time. This means that the marker needs to be thin in at least one dimension.
2) The easiest way to identify a marker in an OCT image is if the material absorbs infrared light (1295 nm wavelength for our system). The marker will appear completely black in the image and the light will not reach the tissue below it, producing a black mark through the image.
3) A marker should not alter the material behavior of the tissue.

Cow and Sheep Tendon (and/or Ligament)

Tendon and ligament from cow or sheep are thick pieces of dense connective tissue. Many materials are suitable for marking them. One method that was not very successful was gluing small pieces of foil to the surface of the tissue. Foil works, but it is very difficult to deal with thin pieces of flimsy foil that crumple easily. A second method considered was inserting small pins across the surface of the tissue, perpendicular to the line of image scanning. For strain tests, I was concerned that the pins may alter the material properties. The pins I had were too big, leaving large holes in comparison to the size of the tissue. Smaller pins may have been acceptable. The best method used on these tissues was adhering a piece of black nylon thread perpendicular to the long axis of the tissue, along which I was imaging. Small pieces of thread were cut to a length about equal to the width of the tissue. The thread was then grasped with tweezers or forceps. A small amount of gel cyanoacrylate (Super Glue) was placed on a smooth surface and the thread was drug through the glue and then dabbed off slightly on a smooth surface before placing it on the tissue. You must be careful to not leave too much glue on the thread because it will show up on the images and will change the properties of the tissue at its location.

Rat Tail Tendon Fascicles

Fascicles are VERY tiny pieces of tissue (~300 micron diameter). Small tissues require small markers. Pins are too large. Foil is too difficult to work with. Thread was used as described above. This worked well, but the thread used was braided which meant that it was made of many small fibers. The fibers sometimes stuck out from the main piece of thread and appeared in the image, making it look messy. Black nylon monofilament thread may have worked better, but none could be found. Blue monofilament polyglyconate suture was finally used. The suture did not completely absorb the light, but its perfectly circular cross-section made it unmistakable in the images. Verhoff's stain was also tried on the fascicles. Thin lines of stain were applied with the edge of a scalpel blade perpendicular to the imaging plane. This did not work. Even though the stain is black, absorbing visible light, it does not absorb infrared light.

Appendix C - Crimp Measurement Procedure

1) Import OCT image set (images of a single fascicle at different strain increments) into Scion Image.
2) If OCT images were pre-logged (saved with the Log option set), you only need to save the files in Scion Image. The saved files will now be in "tif" format.
3) If OCT images were not pre-logged, apply Process -> Arithmetic –Log to each image and then save.
4) Close all the images in Scion Image and exit the program.
5) Open the newly converted "tif" files in Photoshop.
6) Use Image -> Rotate Canvas -> 90° CCW or CW (whichever you like best) to orient the image with the long axis of the fascicle horizontal on the screen.
7) Save.
8) Zoom in to 300 or 400%.
9) Identify an "area of interest" containing at least 3 to 5 consecutive band pairs that are visible through most of the strain increment images that still contain ANY visible band pairs.
10) Change image mode to RGB color (Image -> Mode -> RGB Color).
11) Determine the center of the fascicle on each side of the area of interest using the measure tool (little ruler) to measure the thickness of the fascicle at that point and then divide by two. To see the measurements, make sure the Show Info window is visible.
12) Mark the two center points with single red (or your favorite color) dots.
13) Draw a colored line between the two center points. (You may want to save the images with a new name at this point, in case you want to preserve the original images and the work you've done thus far.)
14) Apply Filter -> Noise -> Median (with a 1 pixel radius) once.
15) Use Image -> Adjust -> Threshold to convert the image to binary (black and white), choosing an "appropriate" threshold value such that bands appear across most of the thickness of the fascicle in the 0% strain image and such that the last increment that has visible banding prior to the threshold, still has visible banding.
16) Apply the same threshold value to each image in the set.
17) Use the measure tool to measure across each bright and dark band pair along the centerline that was created, within the area of interest.
18) Record each measurement viewed in the Info window.

Appendix D – Statistics Resources

I found a wonderful website with a plethora of statistics information (faculty.Vassar.edu/~lowry). There's basically a book on-line that covers the basics and many statistical tests. There are also programs built into the website that will do minimal statistical tests for you.

I also downloaded a demo version of SigmaStat 2.0. You can't save anything in the demo, but you can run many statistical tests and entering the data is easier (especially if it's already in SigmaPlot) than on the website. The SigmaStat demo crashes a lot though.

The statistical test used on the fascicle crimp measurements was a one-way repeated measures analysis of variance (ANOVA). This test is also called a one-way analysis of variance for correlated samples (website).

From the SigmaStat help file "Repeated measures tests are used to detect significant differences in the mean or median effect of treatment(s) within individuals beyond what can be attributed to random variation of the repeated treatments." In the fascicle study, each band pair was considered an "individual" (or subject) and the treatment (or factor or condition) was the level of strain.

The following table shows how the data was organized (only the measurements for the first ten band pairs are shown). The data actually entered into SigmaStat is shown in **bold.**

Individual Band Pair	Treatment (% Strain)				
	0.0%	0.5%	1.0%	1.5%	2.0%
1	**38**	**39**	**43**	**38**	**40**
2	**45**	**42**	**40**	**43**	**33**
3	**13**	**21**	**21**	**17**	**26**
4	**43**	**37**	**38**	**43**	**43**
5	**12**	**13**	**10**		
6	**10**	**11**	**12**	**21**	**24**
7	**13**	**14**	**12**		
8	**15**	**11**	**16**	**28**	**28**
9	**12**	**13**	**10**	**10**	**11**
10	**9**	**11**	**13**	**11**	**9**

In SigmaStat, once the data is entered, if there are missing data points (i.e. blanks for band pairs that disappeared), the blanks need to be converted to missing values (it enters a dash (-) in place of the blank). To do this you go to the Transforms menu, select Missing Values..., and follow the instructions, choosing to replace blanks. Now the statistical tests can be performed on the transformed data. On the Statistics menu choose Repeated Measures → One-way Repeated Measures ANOVA. Choose the Raw Data format. Next select each column of data (each treatment or level of strain) that is to be tested. Finally, press Finish. A repeated measures ANOVA assumes that the data is normally distributed and that there is equal variance. SigmaStat tests these two assumptions before completing the ANOVA. The results will appear in a report. If the normality test fails, the number of samples taken may not be large enough to represent the population. The most important statistic in the report is the P value. For a confidence level of 95% that the treatments have a significant effect, P must be less than 0.05.

Appendix E – Strain & Stress Definitions

Strain is defined as a relative change in shape or size due to externally applied forces.

One-dimensional Engineering Strain (ε) = $\Delta l/lo$,
where Δl = change in length
and lo = the original length.

Stress is the internal force per unit area associated with strain.

Stress (σ) = F/Ao,
where F = force
and Ao = original cross-sectional area (perpendicular to the axis of the force).

Hooke's Law states that stress is directly proportional to strain.

$\sigma = \varepsilon * E$
where E is the elastic modulus.
$E = \sigma / \varepsilon$.

Hooke's Law is valid under low strain conditions for regular elastic materials (like steel). Every material has an elastic limit beyond which permanent (plastic) deformation occurs.

Appendix F – Mechanical Test Device Drawings

Clamp Top

Top View

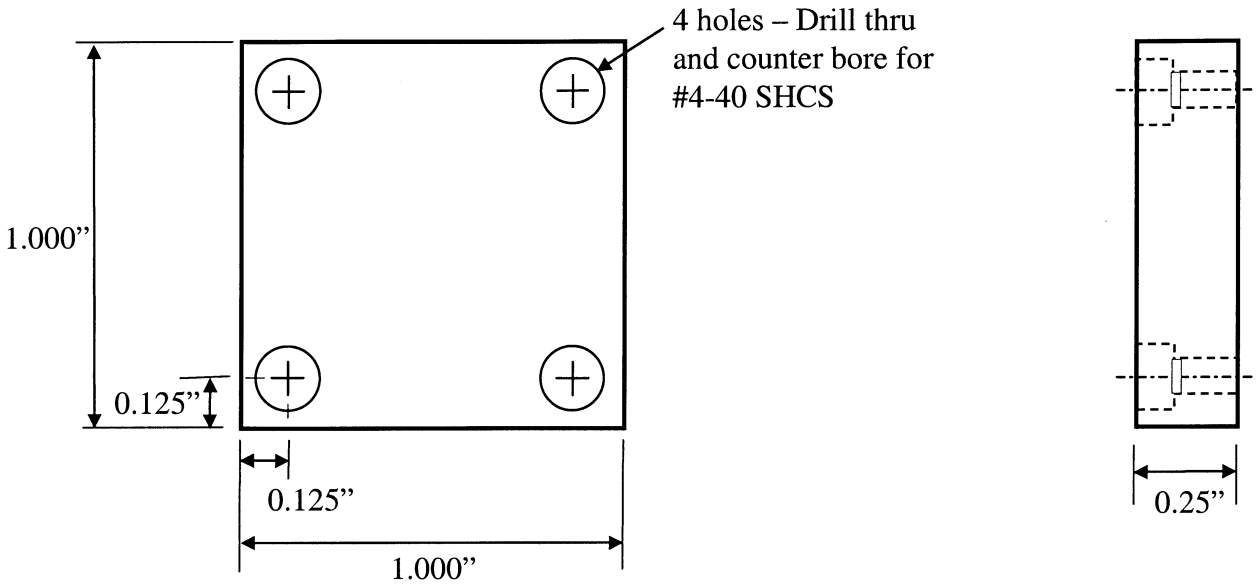

Bottom View

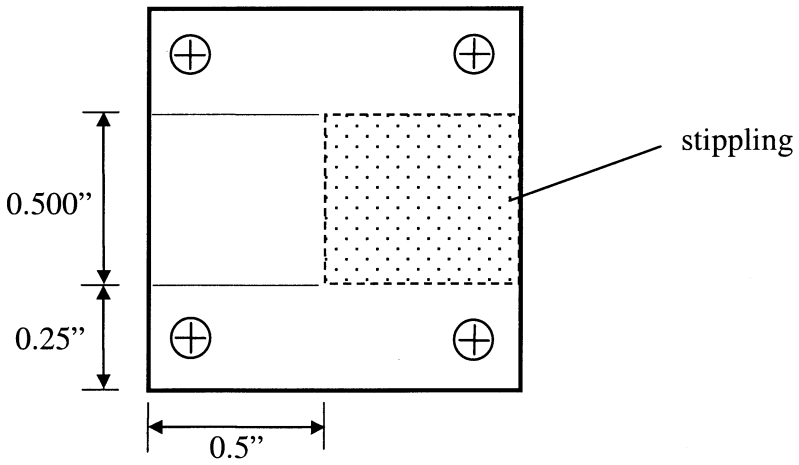

Material: ¼" SS 316 Plate
Notes: Need 2 pieces.
Holes must match up with those in
Clamp Bottom A and B.

Front View

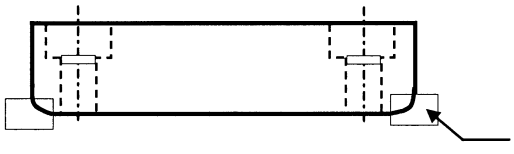

Clamp Bottom A

Top View

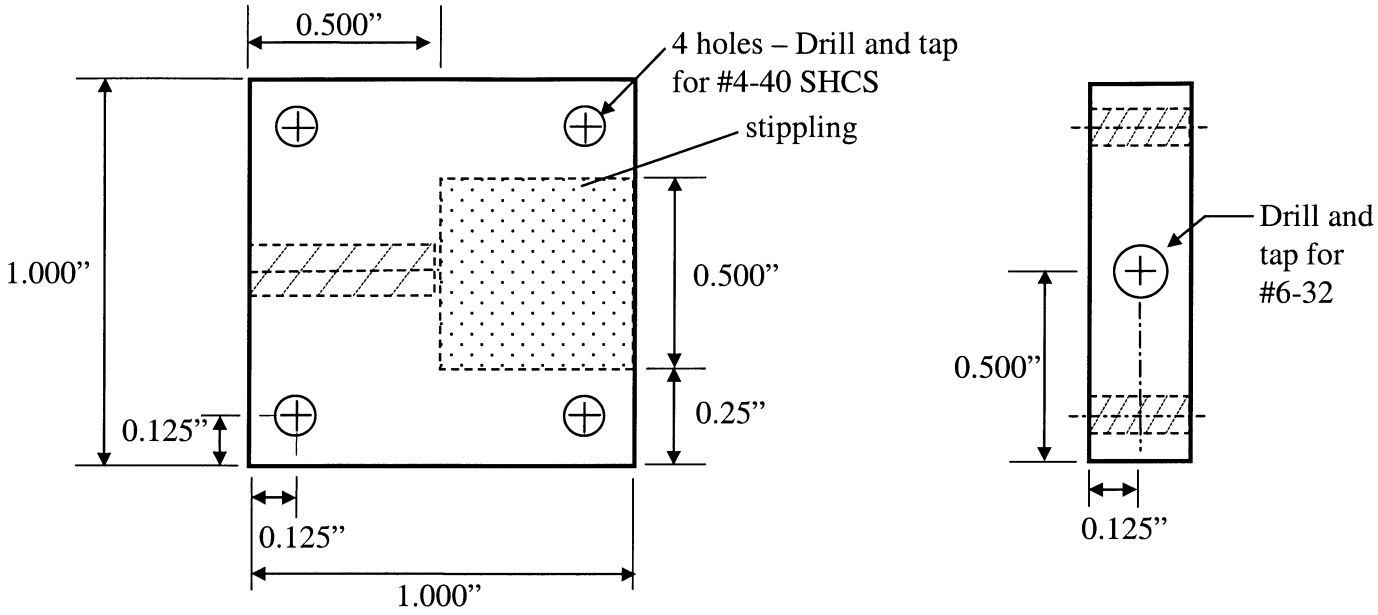

Front View

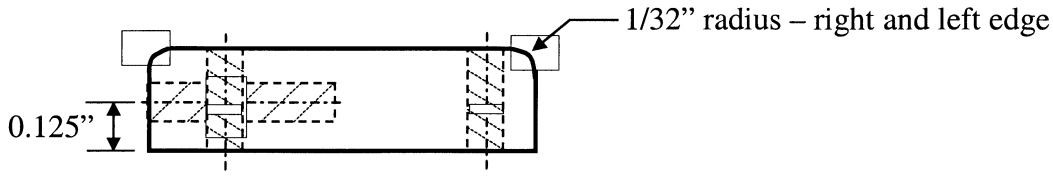

Material: ¼" SS 316 Plate
Notes: Need 1 piece.
4 holes must match to those in Clamp Top.

Clamp Bottom B

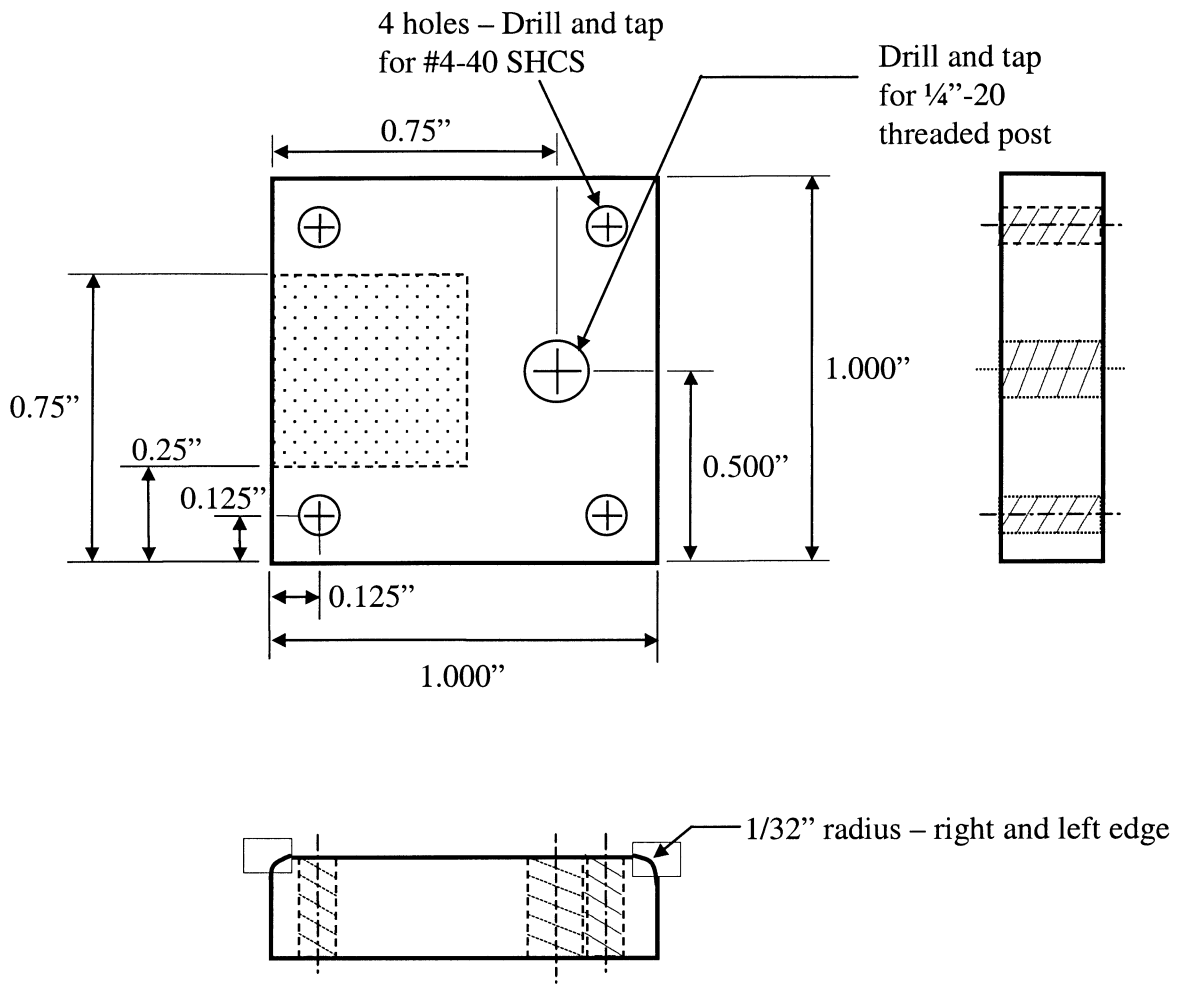

Material: ¼" SS 316 Plate
Notes: Need 1 piece.
4 holes must match to those in Clamp Top.

Threaded Rod

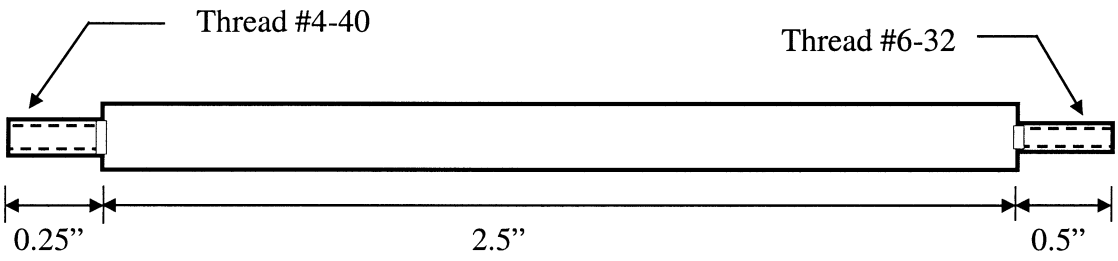

Material: 3/16” Stainless Steel 316 Rod
Notes: Right end (#6-32) screws into Clamp Bottom A. Left end (#4-40) is to be screwed into thread converter and secured.

Thread Converter

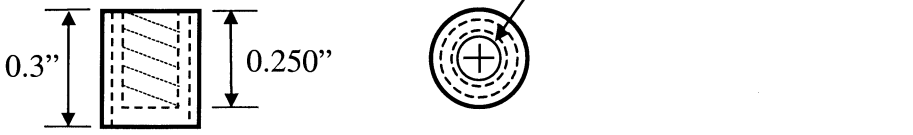

Material: ¼-28 SS all thread rod.
Notes: 0.3" dimension is not critical. Only need 0.250" threaded hole, not thru.
Please attach securely to Threaded Rod.
Also needed: two 2" long all-thread pieces.

Support Plate

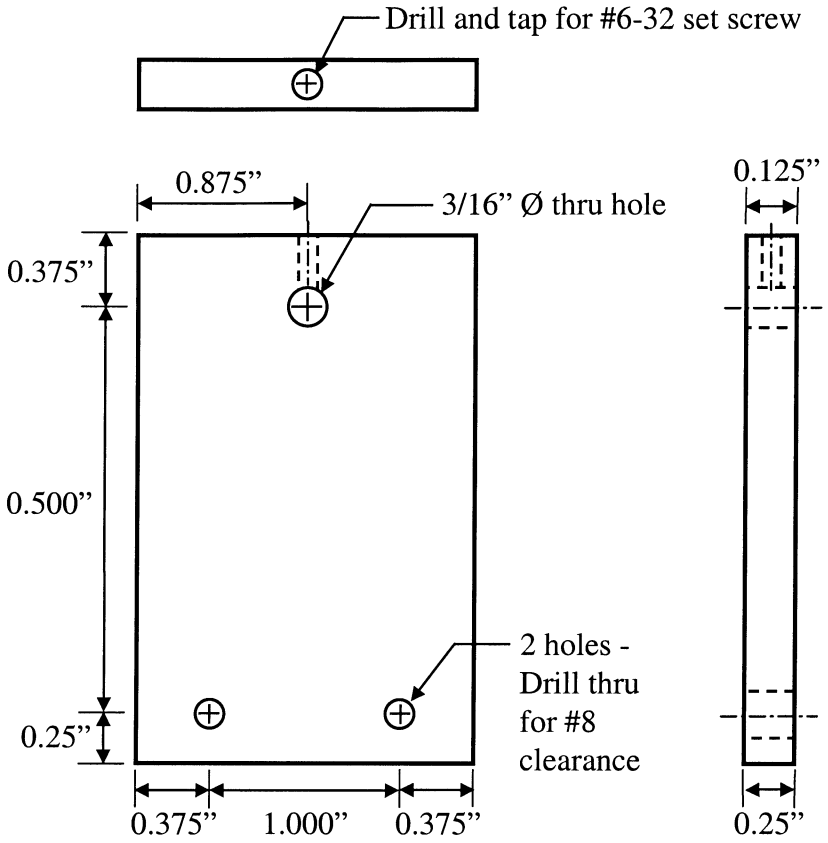

PMMA Box

Bottom Plate

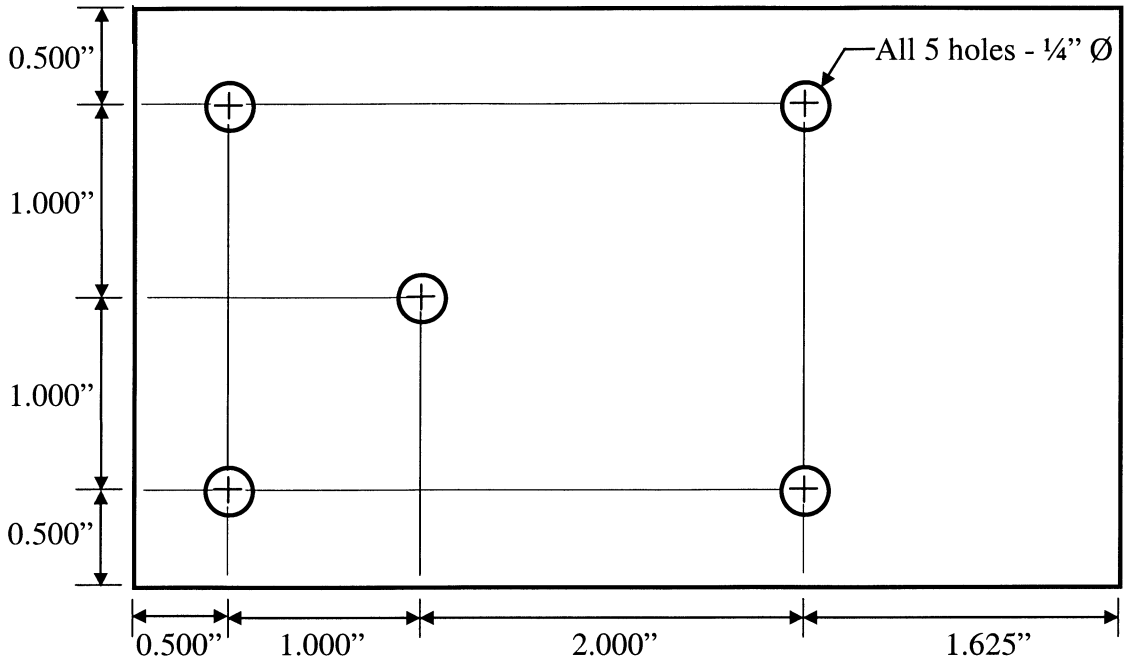

Side A

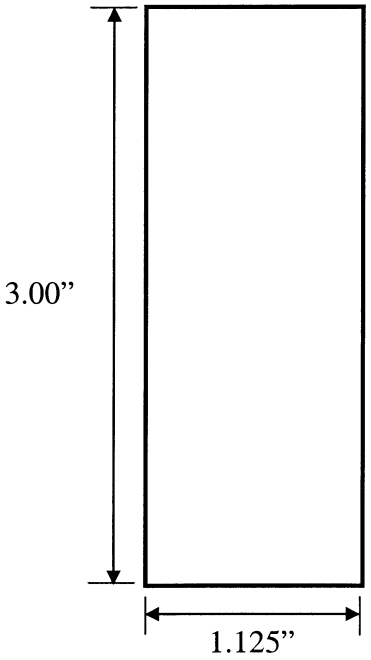

Side B

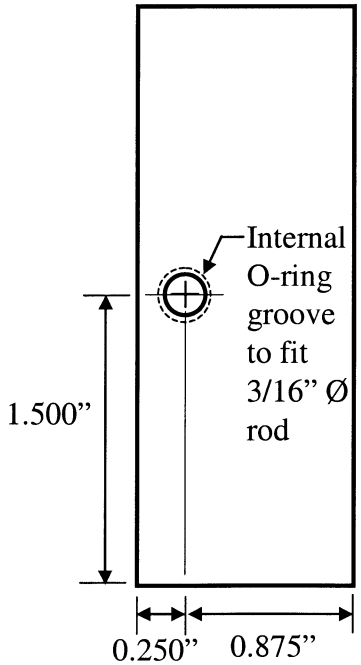

Assembly:

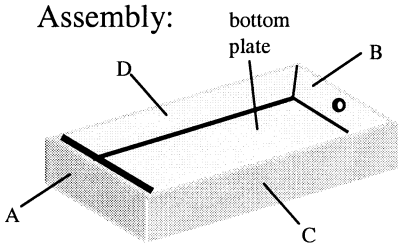

Material: All 1/8" thick PMMA, except side B, which should be ¼" to allow for O-ring groove.

Notes: Please bond box together, hold square, flat, and parallel. Please fit O-ring.

Side C & D (2 pieces)

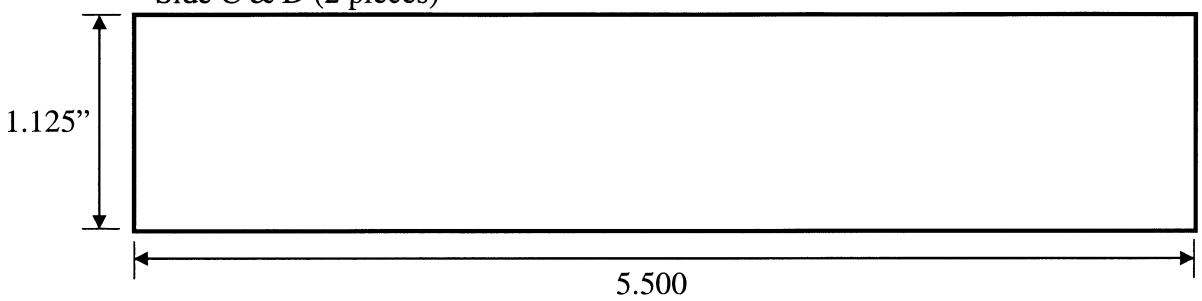

3-D

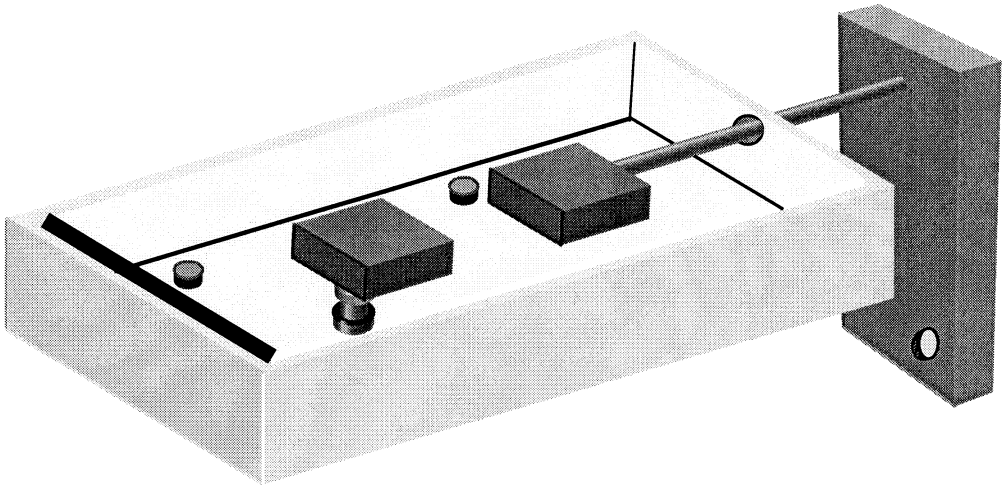

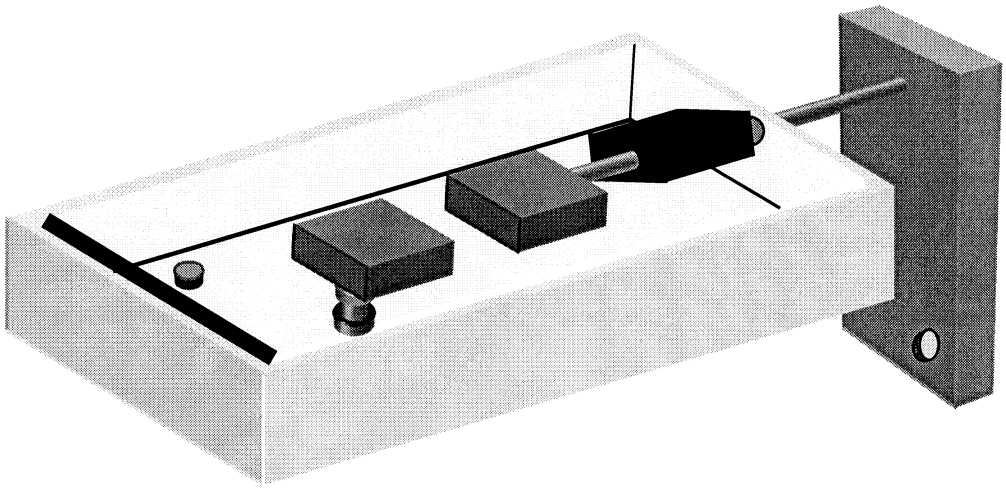

Contacts

- Nelson in the AME machine shop is a wonderful contact for help with any machining needs. He is also a good source for help finding materials.
- 3/16" diameter stainless steel (SS) 316 rod can only be bought in 9-12 foot lengths for a hefty price, except from the UofA machine shop in the Gould Simpson building.
- PMMA was purchased from Cadillac Plastics, which is no longer located in Tucson. Any plastic company should have the needed PMMA.
- ¼" SS 316

Clamp Top

Top View

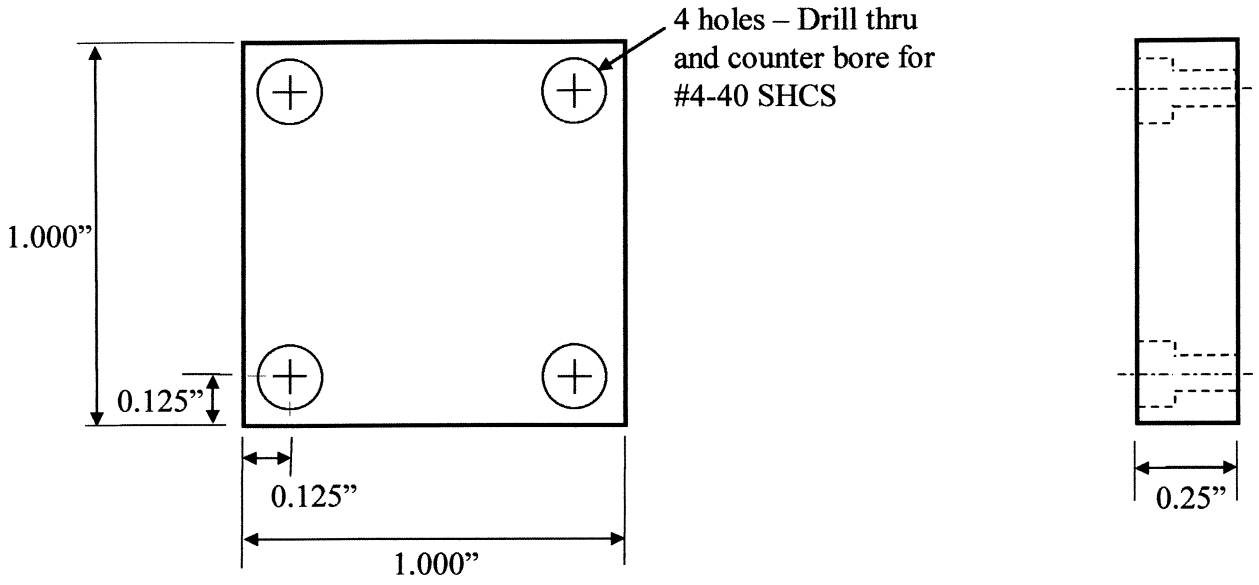

Bottom View

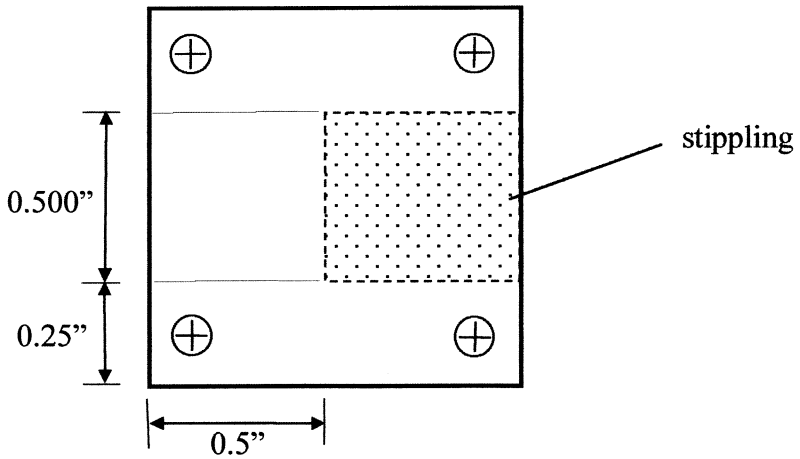

Material: ¼" SS 316 Plate
Notes: Need 2 pieces.
Holes must match up with those in
Clamp Bottom A and B.

Front View

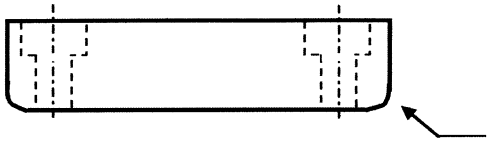

Appendix G – Master's Presentation

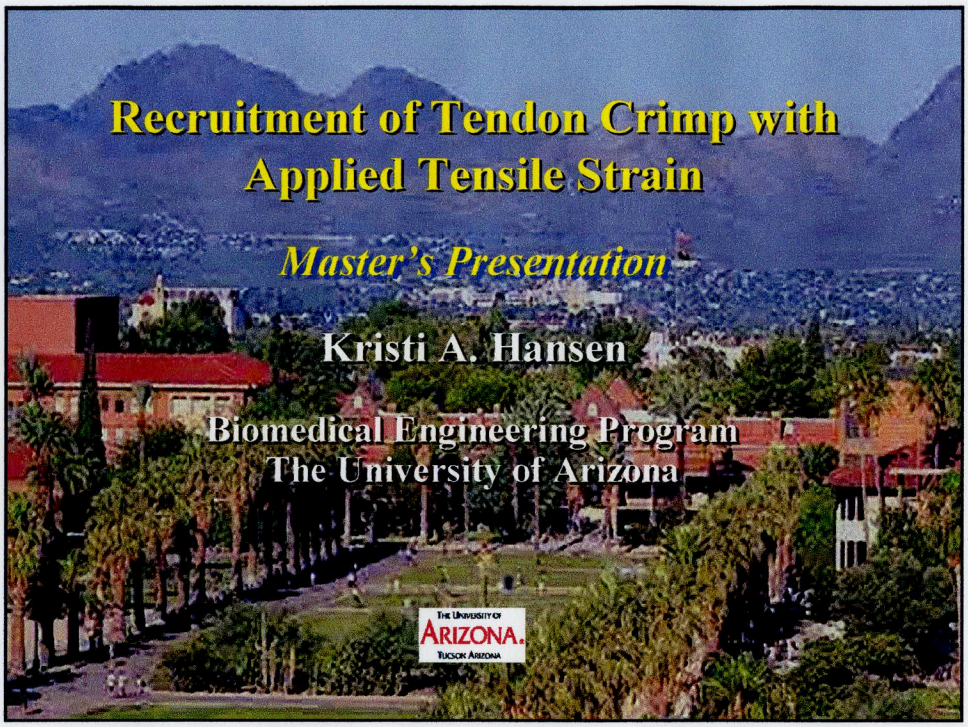

Requirements

- Publication Ready Manuscript
- Supplemental Materials
  - ✓Tissue Marking Techniques
  - ✓Tissue Clamping Technique
  - ✓Crimp Measurement Procedure
  - ✓Statistics Resources
  - ✓Strain & Stress Definitions
  - ✓Mechanical Test Device Drawings
  - ✓Reference Papers for the Lab

Agenda

- Motivation
- Overview of My Research
- Significant Results & Discussion
- Suggestions for Future Work

Motivation

- Why go back to school?
- Why Dr. Barton's lab?
- Why tendons and ligaments?

Motivation

- OCT is new.
- Dr. Barton is easy to work with.
- Applications for clinical use of OCT are waiting to be discovered.
- Everyone (almost) injures a tendon or ligament sometime in their life.

Motivation

- Tissue hierarchy contributes to continuum level material properties.
- Collagen crimp affects material behavior.
- OCT can visualize internal crimp.
- OCT may provide a noninvasive method for evaluation of normal and healing tissues and the efficacy of treatment regimens.
- Technique could be used to determine microstructural parameters for constitutive models of material behavior.

Preliminary Tests
OCT Can Visualize Crimp Pattern

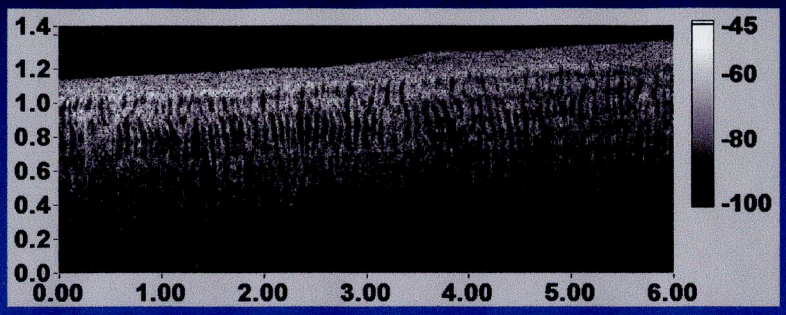

OCT image of bovine ligament.

Imaging Crimp During Stretch

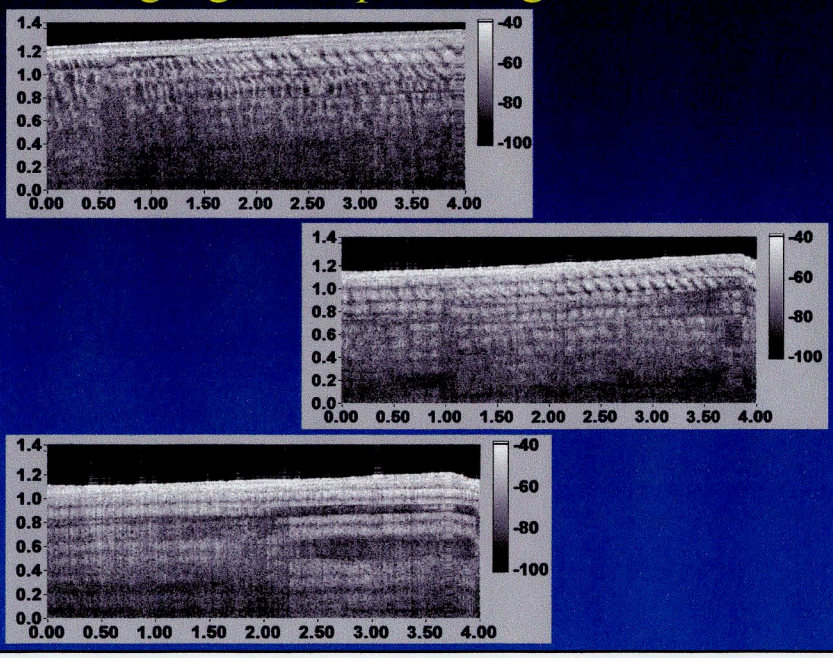

Problems in the Beginning

- Cow ligaments and tendons were too big.
- Could not rely on meat lab for sheep knees.
- 10lb load cell was not sensitive enough for rat tail fascicle tests.
- Amplifying circuit couldn't adjust for load cell imbalance.
- Mechanical test device suffered from friction problems.

Success!

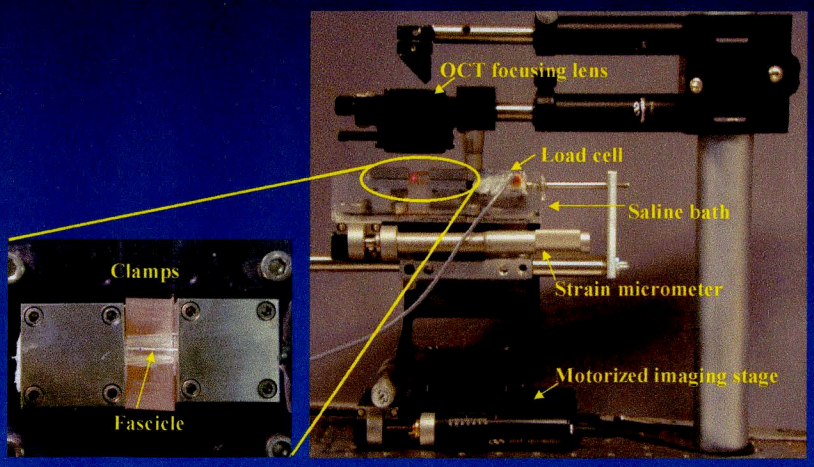

Objective & Hypotheses

- Objectives:
  - Assess the period of the crimp pattern in rat tail tendon fascicles.
  - Measure changes in crimp period as a function of tensile strain using OCT.
- Hypotheses:
  - The width of crimp bands would increase and the bands would eventually disappear as increasing axial strain was applied.
  - The average period of sequential, axially aligned crimp bands would increase with increasing strain.

Organization of Tendons & Ligaments

- Tendons and ligaments have been studied in depth due to their highly organized structure, composed mainly of collagen.

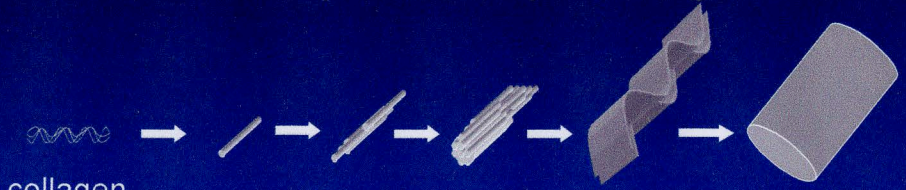

- Collagen exhibits "crimp" or waviness at the structural level of the fascicle.

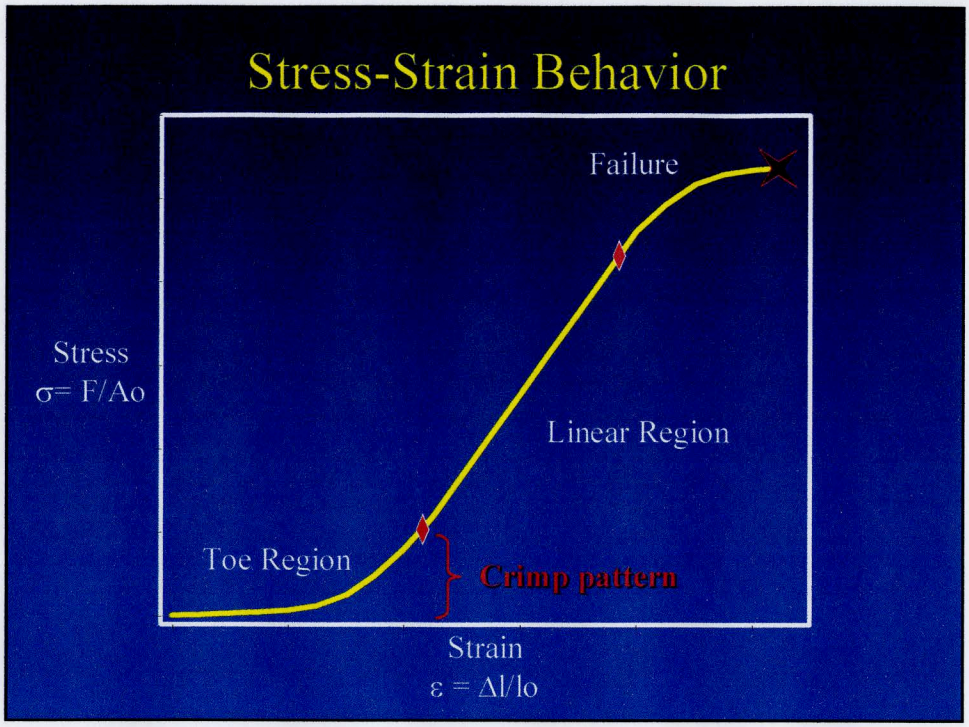

Banding

- Crimp banding has been assessed previously using an optical microscope with polarized light.
- Crimp banding in OCT images has not been been assessed by other researchers.
- Birefringent OCT banding has been assessed by other researchers.

OM Studies of Crimp

- Diamant saw crimp pattern in mildly disintegrated rat tail tendons using a transmitted polarized light microscope.

- Banding is caused by periodic variation in orientation within the birefringent fibers. In OM banding is a birefringence affect.

Birefringence

- Collagen is a birefringent material.
- The polarization state of light is rotated.
- PS-OCT has been used to image birefringent banding that indicates tissue state or organization.

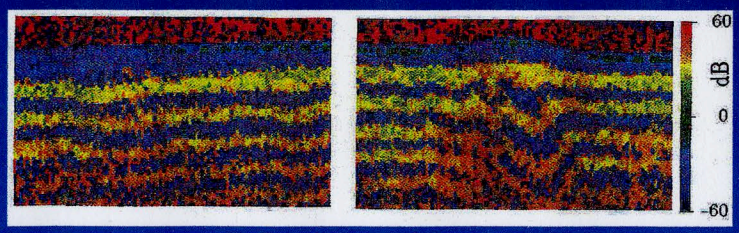

Bovine tendon

Methods

- Fascicles were teased from rat tail sections and gripped in stainless steel clamps mounted in a custom-built stretching device.
- Zero-load length determined by consecutively applying and removing a small tare load and measuring with calipers.
- Images were acquired at ½% strain increments until banding disappeared, after allowing load to relax.
- Crimp period was measured using image analysis software.
- OM and OCT images were compared.

Results

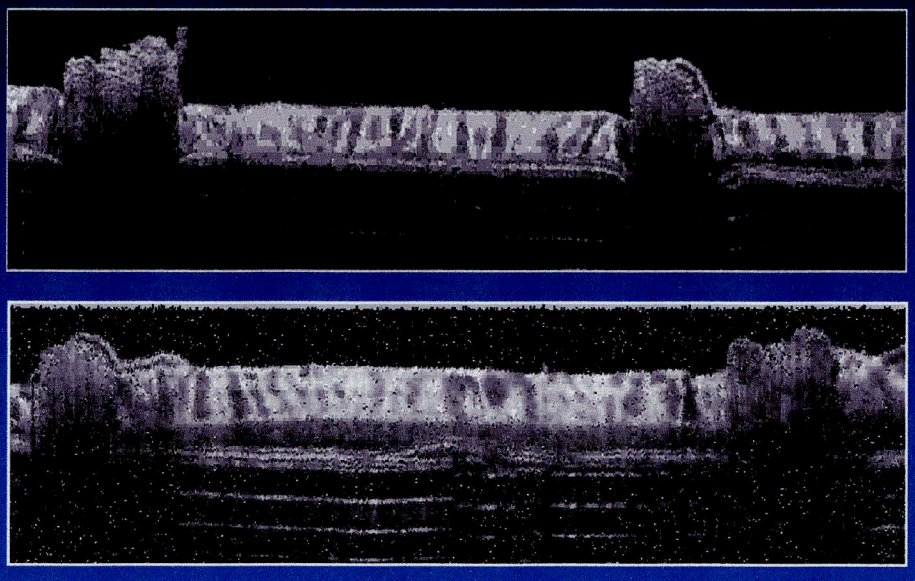

Average Stress-Strain Curve for Rat Tail Fascicle

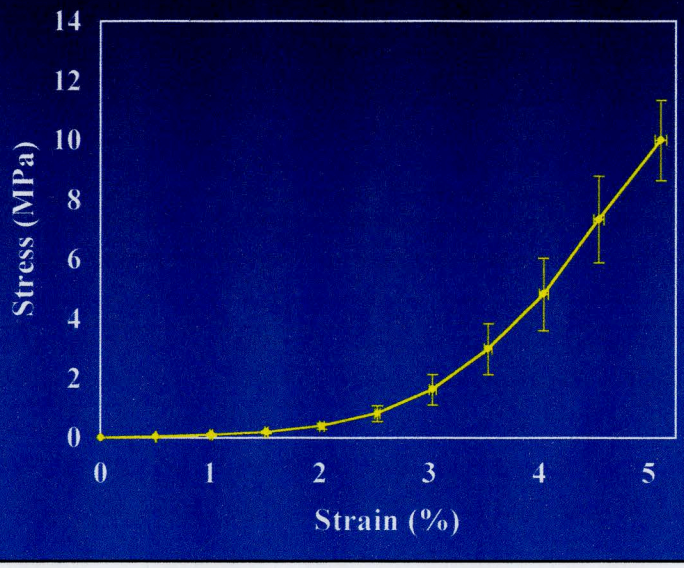

OCT/OM Comparison

OCT crimp band image

OM crimp band image

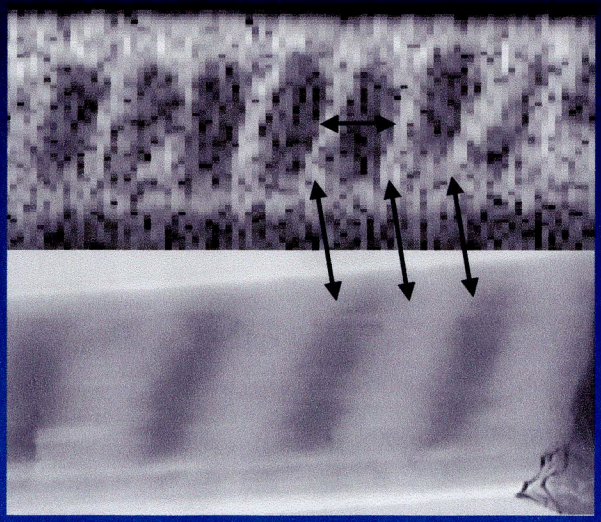

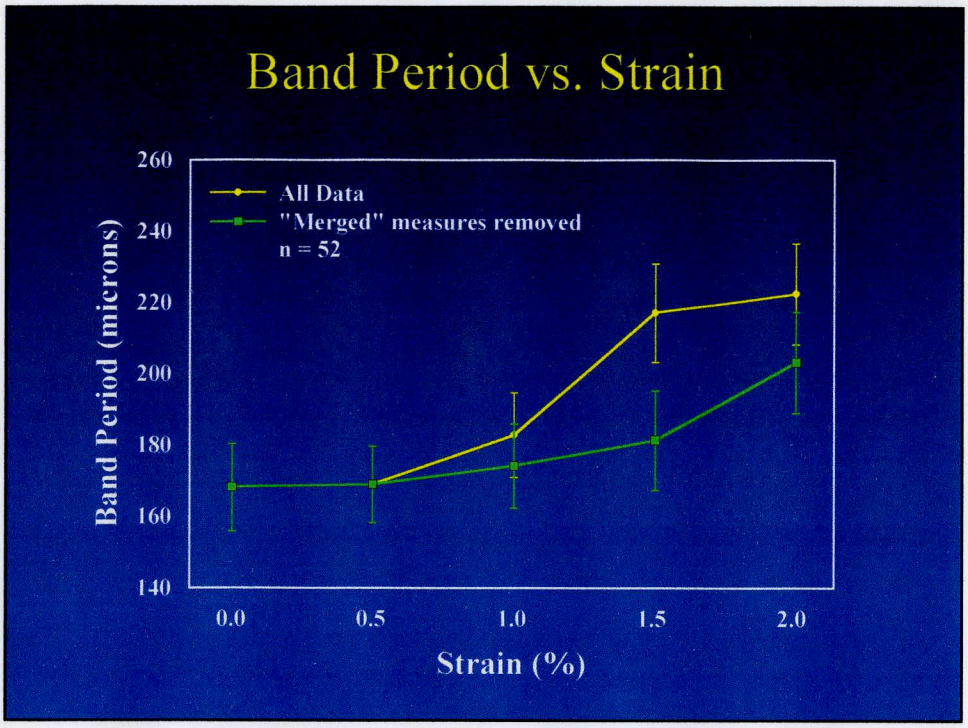
Band Period vs. Strain
260
240
220
200
180
160
140
Band Period (microns)
All Data
"Merged" measures removed
n = 52
0.0
0.5
1.0
1.5
2.0
Strain (%)

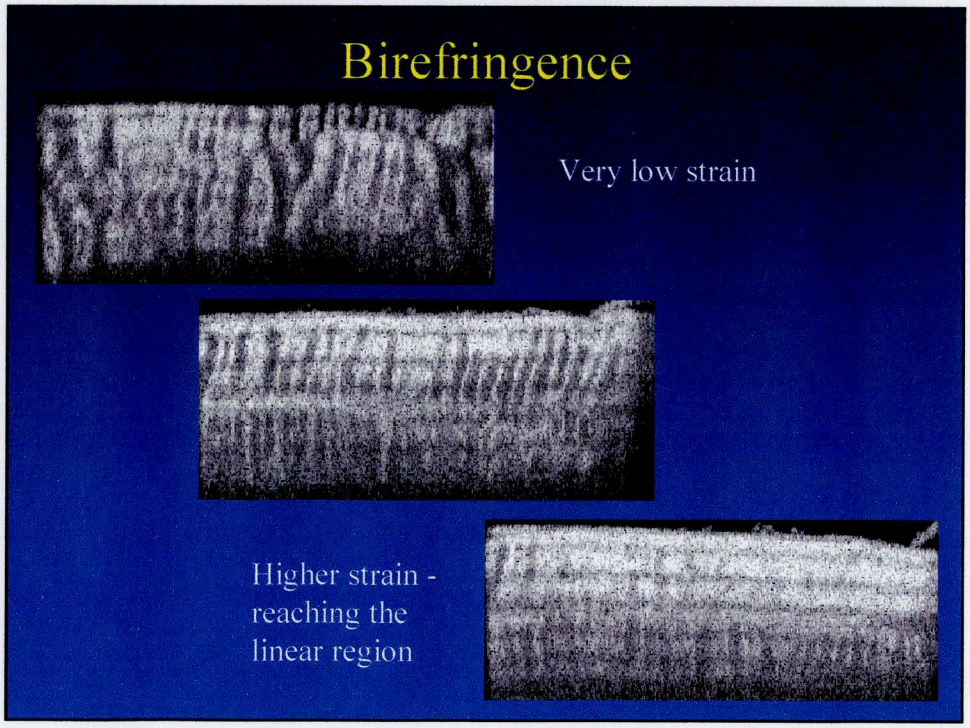
Birefringence
Very low strain
Higher strain - reaching the linear region

Limitations

- 15 micron resolution
- Possible migration of tissue during stretching
- Load cell sensitivity
- Noisy images and time consuming measurements.

Possible Future Work

- Clinical applications: Catheter for arthroscopy to look at collagenous tissue damage and repair.
- Stress relaxation imaging.
- Volumetric strain images.
- Combined analysis of crimp period and birefringent banding.

Appendix H – Strain Sequence OCT Images

0% Strain

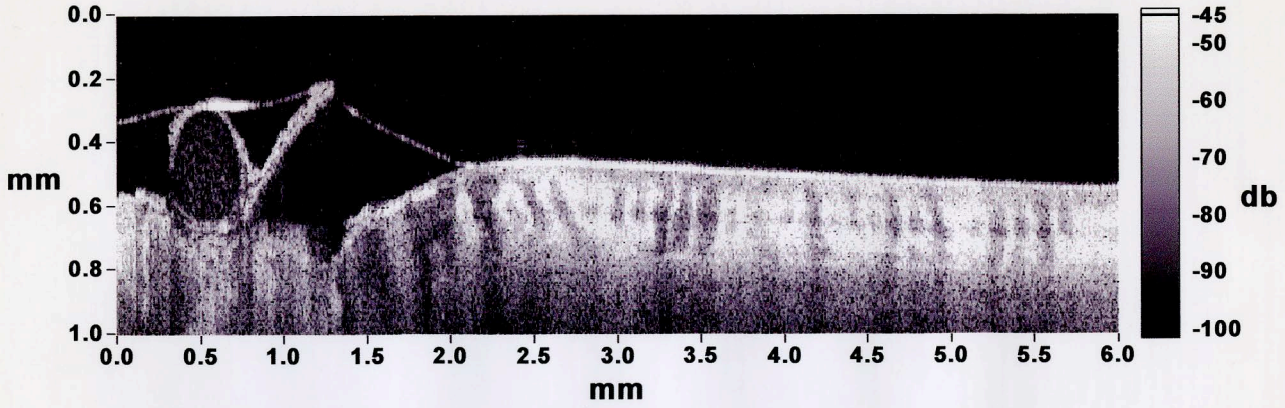

0.5% Strain

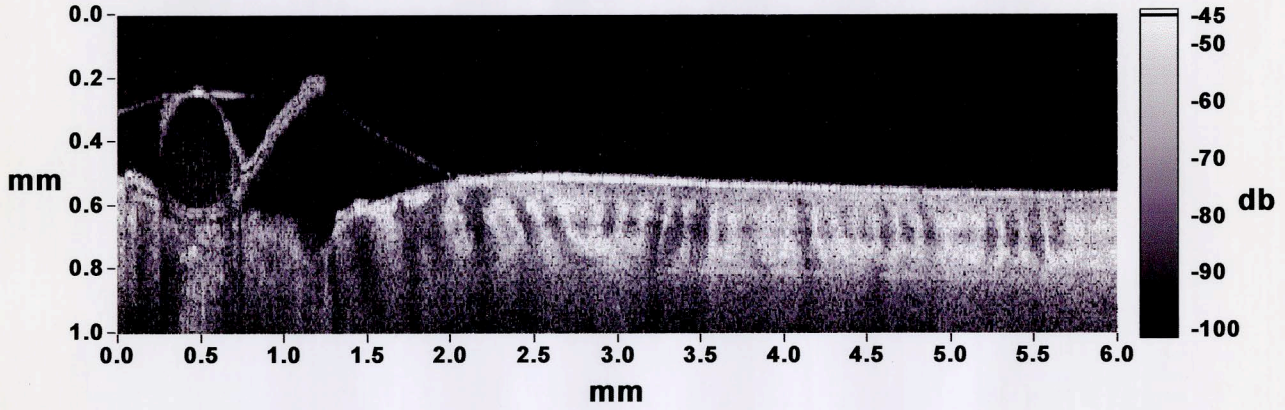

1.0% Strain

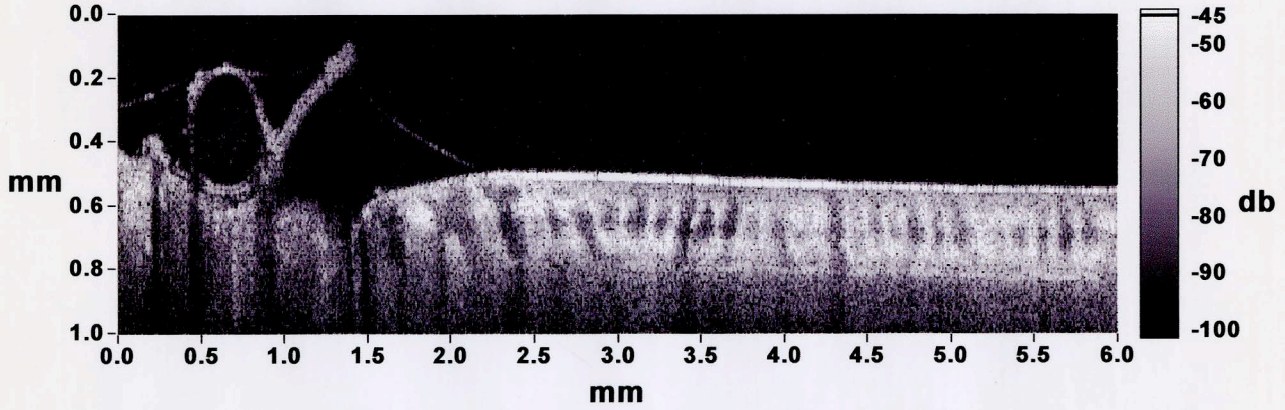

1.5% Strain

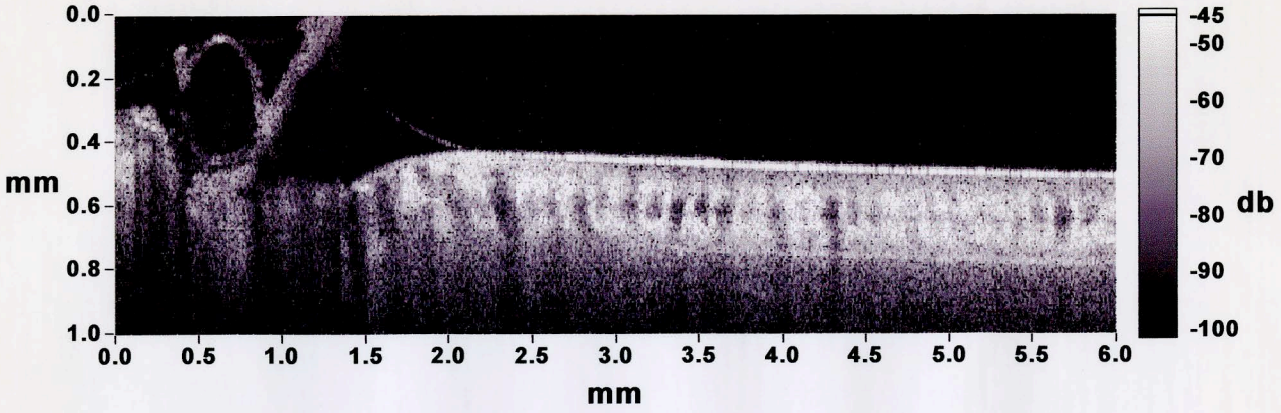

2.0% Strain

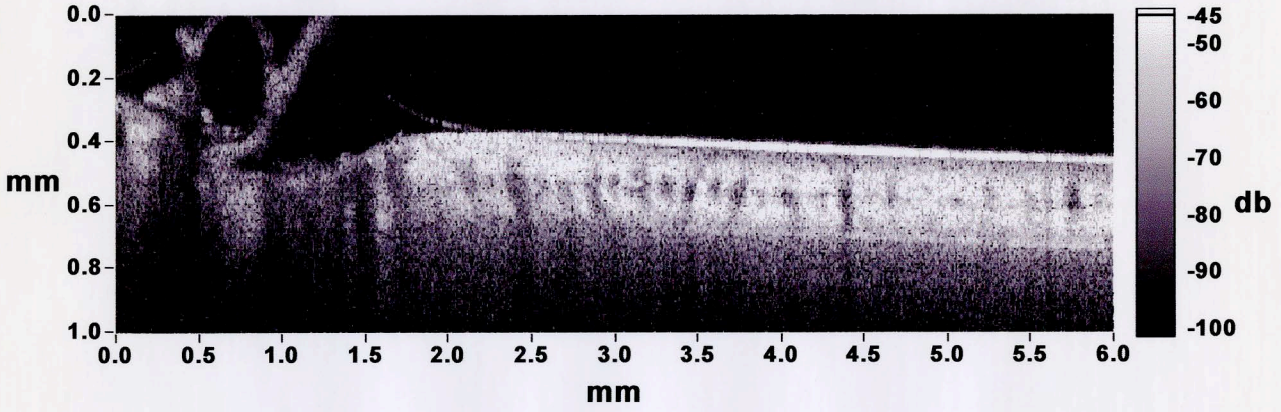

2.5% Strain

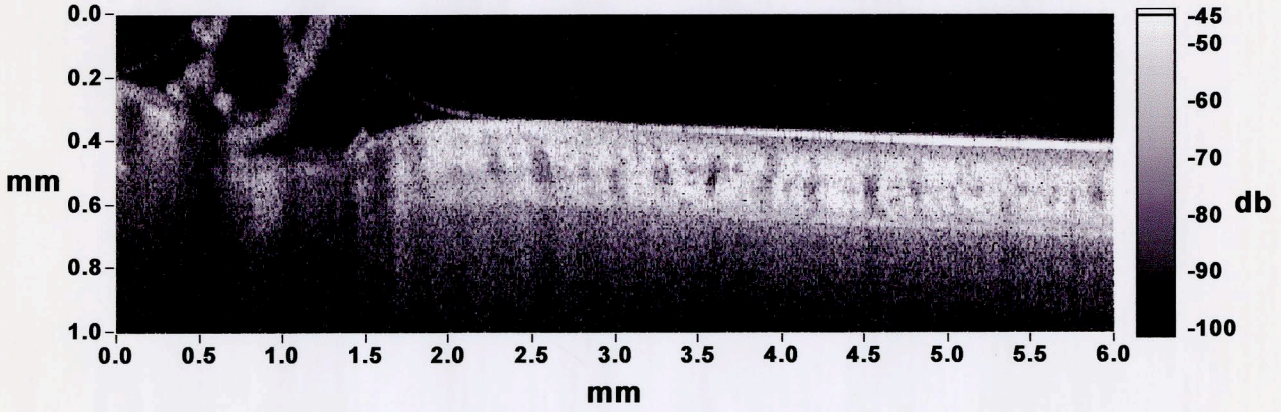

3.0% Strain

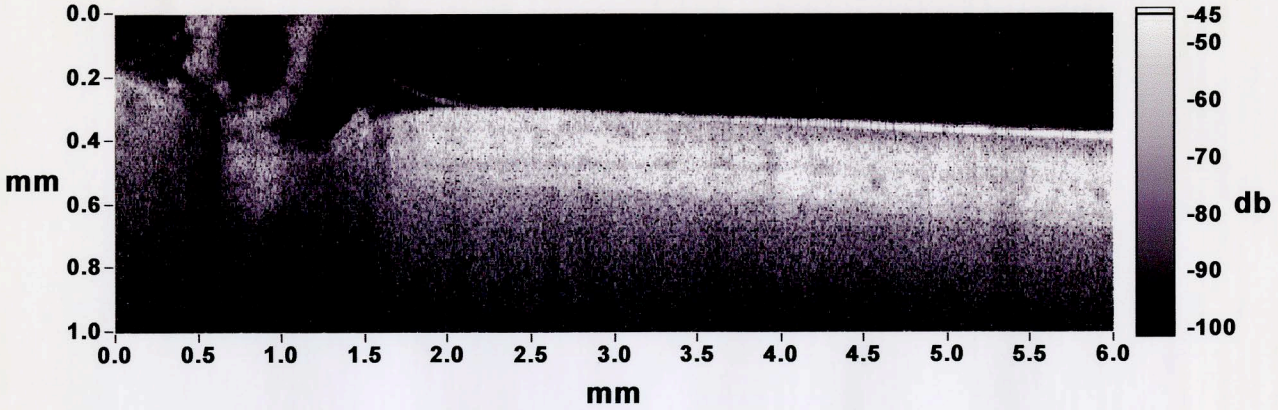

3.5% Strain